Predominant floodplain over mountain weathering of Himalayan sediments (Ganga basin)

Maarten LUPKER[1*], Christian FRANCE-LANORD[1], Valier GALY[2], Jérôme LAVÉ[1], Jérôme GAILLARDET[3], Ananta Prasad GAJUREL[4], Caroline GUILMETTE[1], Mustafizur RAHMAN[5], Sunil Kumar SINGH[6], Rajiv SINHA[7]

[1]Centre de Recherches Pétrographiques et Géochimiques (CRPG-CNRS), 15 rue Notre Dame des Pauvres, 54501 Vandoeuvre les Nancy, France.

[2]Woods Hole Oceanographic Institution (WHOI) - Department of Marine Chemistry and Geochemistry, 266 Woods Hole Rd., Woods Hole, MA 02543, USA.

[3]Institut de Physique du Globe (IPGP), 1 rue Jussieu, 75238 Paris, France.

[4]Department of Geology, Tri-Chandra Campus, Tribhuvan University, Kathmandu, Nepal.

[5]Department of Soil Science, University of Dhaka, Bangladesh.

[6]Physical Research Laboratory (PRL), Navrangpura, Ahmedabad, 380009, India.

[7]Engineering Geosciences Group, Indian Institute of Technology (IIT), Kanpur, 208016, India.

*Corresponding author: mlupker@crpg.cnrs-nancy.fr

Abstract

We present an extensive river sediment dataset covering the Ganga basin from the Himalayan front downstream to the Ganga mainstream in Bangladesh. These sediments were mainly collected over several monsoon seasons and include depth profiles of suspended particles in the river water column. Mineral sorting is the first order control on the chemical composition of river sediments. Taking into account this variability we show that sediments become significantly depleted in mobile elements during their transit through the floodplain. By comparing sediments sampled at the Himalayan front with sediments from the Ganga mainstream in Bangladesh it is possible to budget weathering in the floodplain. Assuming a steady state weathering regime in the floodplain, the weathering of Himalayan sediments in the Gangetic floodplain releases ca. $(189 \pm 92)\cdot10^9$ and $(69 \pm 22)\cdot10^9$ moles/yr of carbonate bound Ca and Mg to the dissolved load, respectively. Silicate weathering releases $(53 \pm 18)\cdot10^9$ and $(42 \pm 13)\cdot10^9$ moles/yr of Na and K while the release of silicate Mg and Ca is substantially lower, between ca. 0 and $20\cdot10^9$ moles/yr. Additionally, we show that sediment hydration, $[H_2O^+]$, is a sensitive tracer of silicate weathering that can be used in continental detrital environments, such as the Ganga basin. Both $[H_2O^+]$ content and the D/H isotopic composition of sediments increases during floodplain transfer in response to mineral hydrolysis and neoformations associated to weathering reactions. By comparing the chemical composition of river sediments across the floodplain with the composition of the eroded Himalayan source rocks, we suggest that the floodplain is the dominant location of silicate weathering for Na, K and $[H_2O^+]$. Overall this work emphasizes the role of the Gangetic floodplain in weathering Himalayan sediments. It also demonstrates how detrital sediments can be used as weathering tracers if mineralogical and chemical sorting effects are properly taken into account.

1. INTRODUCTION

Chemical weathering is central in surface biogeochemical cycles because it redistributes the chemical elements between Earth's surface reservoirs such as continental crust and the Ocean. Over geological timescales, silicate weathering coupled with carbonate precipitation in the Ocean is responsible for a large fraction of atmospheric sequestration that balances the mantle and metamorphic CO_2 inputs into the atmosphere and therefore regulates the global climate (e.g. Walker et al., 1981; Berner et al., 1983). These considerations have fostered research from small-scale mineral dissolution studies (e.g. Oelkers and Schott, 1995; White and Brantley, 2003) to global scale weathering models (e.g., Berner, 1994; Donnadieu et al., 2004). While modern weathering rates are often derived from river solute fluxes (e.g. Meybeck, 1987; Gaillardet et al., 1999a; West et al., 2005), their solid counterparts have received far less attention (e.g. Gaillardet et al., 1999b; France-Lanord and Derry, 1997; Gislason et al., 2006) probably because of the difficulty of integrating the variability of detrital sediments over space and time (Lupker et al., 2011; Bouchez et al., 2011a; 2011b; 2011c). Sediment records are however one of the rare archives that can be reliably used to trace past erosion fluxes at regional scales.

In an effort to understand and quantify the link between the chemical composition of river sediments and chemical weathering, we present a study of modern sediments within the Ganga fluvial network. Silicate weathering within the Himalayan system – the largest active orogen and highest mountain range on Earth - has retained much attention (e.g. Raymo et al., 1988; Derry and France-Lanord, 1996; Galy and France-Lanord, 1999) as it is commonly assumed that chemical weathering is directly associated with physical erosion, triggered by relief and elevation. However, the spatial budget and *locus* of weathering within the

Himalayan system has never been properly determined, even though a predominant role of the floodplain compartment in the weathering budget of the Himalayan system has been proposed (Galy and France-Lanord, 1999; West et al., 2002). The Ganga River system is draining the central-western part of the Himalayan orogen where high erosion rates are responsible for large sediment load (c.a. 400-500 Mt/yr for the Ganga in Bangladesh, RSP, 1996; Lupker et al., 2011) that transit through an extensive floodplain before being discharged to the Indian Ocean. Heretofore, the role of this extensive floodplain in the chemical weathering process has remained poorly constrained.

We characterize the weathering signature of river sediments collected in the floodplain, along a transect from the Himalayan front downstream to the outflow of the Ganga in Bangladesh and further compare these sediments to the Himalayan source rocks. We use mobile to immobile ratios of major elements, carbonate content and hydration of sediments (hereafter referred to as [H_2O^+]) to trace and quantify chemical weathering. Sediment hydration marks the uptake of protons by hydrolysis or neo-formation of hydroxyl-rich secondary minerals and can therefore be used as weathering tracer. Additionally, the hydrogen stable isotopic composition (D/H) of the hydroxyl groups reflects the isotopic composition of the water from which they were formed (Savin and Epstein, 1970; Lawrence and Taylor, 1971, 1972; Gilg and Sheppard, 1996) and can potentially be used as a tracer for the weathering locus.

2. STUDY SETTING

2.1. Hydrological and erosional setting

The Ganga River system is mainly fed by tributaries draining the Himalayan range. From west to east, the Yamuna, the Ganga, the Karnali, the Narayani and the Kosi are all major rivers draining the Himalayan range with basin size ranging from 7600 km^2 for the Yamuna to 57800 km^2 for the Kosi. The three main Nepalese Himalayan Rivers (Karnali, Narayani and Kosi) join the Ganga mainstream after a long transit (200 to 600 km) in the Indogangetic floodplain, where the Karnali and Narayani are respectively renamed Ghaghara and Gandak. The westernmost Himalayan tributaries of the Ganga, the Yamuna drains through the city of Delhi and merges with the Ganga in Allahabad, ca. 900 km downstream of the Himalayan front (Figure 1).

Non Himalayan Rivers also contribute to the sediment and dissolved load of the Ganga, in particular southern tributaries. The Chambal River – the largest southern tributary of the Ganga (Rengarajan et al., 2009) – is draining the front of the Vindhya Range and part of the Deccan traps and joins the Yamuna River in the Gangetic plain (Figure 1). After a total transit in the floodplain of ca. 1500 km the Ganga merges with the Brahmaputra, which drains the eastern part of the Himalaya and the southern border of the Tibetan plateau. The confluence of the Ganga and Brahmaputra in Bangladesh forms the Lower Meghna that delivers the products of Himalayan erosion to the Bay of Bengal and the Indian Ocean. The total drainage area of the Ganga covers 1.06 million km^2 of which 17% lies in the Himalaya, 35% in the Indian shield and 48% in the Ganga plain (Rao, 1979).

The major part of the 380 km^3 Ganga's yearly discharge (WARPO hydrological data) occurs during the monsoon season from June to September (Fasullo and Webster, 2003), and approximately 54 % of this discharge is derived from the Himalayan catchments, 22% from the southern tributaries and the remaining 24 % from the floodplain itself (Rao, 1975; Singh et al., 2008). The sediment flux exported by the Ganga is estimated at ca. 400 to 500 Mt/yr of which 90 to 95 % is transported during the monsoon (RSP, 1996; Lupker et al., 2011). Less

than 10% of the eroded Himalayan flux is stored in the Gangetic floodplain (Lupker et al., 2011).

2.2. Geological setting

The Himalayan crust is commonly divided in four main east-west striking geological units. From north to south: the Tethyan Sedimentary Series (TSS), the High Himalaya Crystalines (HHC), the Lesser Himalaya (LH) and the Siwaliks. These units are bound by major faults: the South Tibetan Detachment (STD) between the TSS and HHC; the Main Central Thrust (MCT) between the HHC and LH; the Main Boundary Thrust (MBT) between the LH and Siwaliks and the Main Frontal Thrust (MFT) at the southern front of the range. The TSS are composed of weakly metamorphosed, carbonate rich, late Cambrian to Eocene marine sedimentary sequences. The HHC are formed by Neoproterozoic to Ordovician high grade metamorphic rocks, marbles and local intrusions of leucogranite. The LH are low-grade mostly sedimentary rocks composed of quartzites, phyllites, black shists to limestones, or orthogneiss. To the south, the Siwalik consists of Neogene floodplain deposits uplifted by the southern propagation of the deformation front. Thanks to contrasted signatures of HHC and LH units in Sr and Nd isotopic compositions, Galy and France-Lanord (2001) estimated that 80% of the sediments eroded from the Himalayas are derived from the HHC, and the remaining 20% of the LH, even though river incision (Lavé and Avouac, 2001) or lithology of transported pebble (Attal and Lavé, 2006) show that TSS and Siwalik sediments may also represent a significant part of the eroded material in central Nepal.

Further south, the Himalayan front is bound by the 200 to 300 km wide Ganga. foreland basin. Below the Ganga alluvial plain, several kilometers of sediments eroded from

the Himalayan range overlay the Archean to Early Proterozoic Indian craton (Lyon-Caen and Molnar, 1983).

In the southern part of the basin, the Chambal River drains very different lithologies compared to Himalayan Rivers. The Chambal headwaters and its tributaries are draining the Cretaceous tholeiitic lava flows of the Deccan Traps that cover a significant part of the drainage area and Neoproterozoic to Paleoproterozoic marine deposits mainly composed of sandstones and limestone (Rengarajan et al., 2009 and references therein).

3. SAMPLING STRATEGIES AND ANALYTICAL PROCEDURES

3.1. River sediment sampling

Rivers in the Ganga basin were repeatedly sampled mainly during the monsoon season, in 2001, 2002, 2004, 2007, 2008, 2009 and 2010. All major tributaries of the Ganga in Nepal, India and Bangladesh were sampled over these 7 years of field campaigns. When possible, sediments were sampled along vertical depth profiles to document the chemical heterogeneity and derive accurate average chemical compositions of the transported material. The main trans-Himalayan tributaries of the Ganga, from east to west: the Yamuna, the Ganga, the Karnali, the Narayani and the Kosi River were sampled at the front of the Himalayan range near the MFT. Additionally, samples from the Eastern and Central watersheds of the Karnali River (Bheri and upper Karnali) near the MBT (upstream of the MFT) were included in this study. The trans-Himalayan Rivers (Ganga, Karnali, Narayani and Kosi) were sampled further downstream in the floodplain, before their confluence with the mainstream Ganga or another major river (except for the Yamuna that was sampled after its confluence with the Chambal). The contribution of Siwalik sediments to the sediment load

was characterized using samples from the Rapti River - a tributary of the Karnali draining mainly Siwalik units - and from more minor tributaries such as the Suraï, Tinau and Rapti Chitwan. The Chambal River, the main river draining the southern part of the Ganga basin, was sampled upstream its confluence with the Yamuna. The Gomti River, disconnected from any direct Himalayan input (Singh et al., 2005) was used as an analogue for pure floodplain sediment input in the Ganga basin. The Ganga mainstream was also sampled in Varanasi (Benares) and Patna in the floodplain. Finally, the Ganga mainstream was repeatedly sampled during the monsoon season (2002, 2004, 2007, 2008 and 2010) at Harding Bridge (Bangladesh). This station located before the confluence of the Ganga with the Brahmaputra integrates all major tributaries contributions to the Ganga River load (Figure 1).

Sampling included: (1) suspended sediment depth profiles in the water column that allow to capture the full sedimentological variability, (2) dredged bedload samples and (3) recent flood deposits or bank sediments. The detail of sampling techniques and preparation can be found in (Galy et al., 2008; Lupker et al., 2011). Part of the sampling presented in this work have already been used to document organic carbon fluxes (Galy et al., 2007; 2008), residence and transfer times in the Ganga basin (Granet et al., 2007; 2010), mineralogical variability (Garzanti et al., 2010; 2011) and to budget global sediment fluxes and composition (Lupker et al., 2011).

3.2. Sample analysis

Major elements, carbonate content and sediment hydration where determined to characterize the weathering signature of exported river sediments.

3.2.1. Major elements

Sediments were first powdered in an agate mortar. Major element concentrations were measured by ICP-AES and ICP-MS at "Service d'Analyse des Roches et des Minéraux" (SARM – CRPG, Nancy-France) on bulk aliquots of ~ 100 mg of sediment after lithium metaborate fusion (Govindaraju and Mevelle, 1987; Carignan et al., 2001). The relative uncertainty for major elemental concentration is better than 2%.

3.2.2. Carbonate content determination

Carbonates contents were manometricaly determined from the CO_2 released after reaction with H_3PO_4 with 30 to 50 mg sample on a manual vacuum extraction line. Calcite was determined after 3 hr at 25°C, and dolomite content was sequentially determined after additional 7 days reaction at 50°C (Sheppard and Schwarcz, 1970; Galy et al., 1999). The isotopic compositions of calcite and dolomite where measured on the released CO_2 by a modified VG-602 mass spectrometer and are reported using $\delta^{18}O$ (SMOW) and $\delta^{13}C$ (PDB) notations. The reported reproducibility is ± 0.1 ‰.

3.2.3. Hydration and D/H stable isotopic composition in sediments

Existing methods for D/H analysis in rocks (Sharp et al., 2001; Gehre and Strauch, 2003; Gong et al., 2007; Garzione et al., 2008) were adapted to analyze detrital, clay rich sediments and to ensure a high sample throughput. Between 2 to 8 mg of powdered sample were analyzed on-line using an Elemental Analyzer (EA) coupled to a VG Isoprime Isotope Ratio Mass Spectrometer (IRMS). Details of the analytical procedure are given bellow.

First, adsorbed and inter-layer water needs to be removed. No general consensus on

200 the elimination procedure of adsorbed water can be found in the literature. Proposed
201 procedures have explored heating the sample to 250°C under vacuum for 2 to 3 hours (Savin
202 and Epstein, 1970), 200°C for 12 hours (Girard et al., 2000), 350°C for 4 hours (Gong et al.,
203 2007) or 70°C under vacuum for 20 days (Garzione et al., 2008). Yapp and Pedley (1985) and
204 Girard et al. (2000) also used up to 3 hours pumping at 100°C to remove exchangeable water
205 from natural goethites. In our procedure, samples were pre-weighted in tin capsules, placed in
206 a sample carrousel and degassed at 120°C under vacuum for 48h in a degassing canister.
207 Great care was taken to use constant degassing temperature and time for all samples to ensure
208 internal reproducibility of the data. Degassing for less than 48h resulted in higher variability
209 in sample water content and isotopic composition that was attributed to remaining adsorbed
210 water. After dehydration, the degassing canister was placed in a dry, N_2 flushed, glovebox. In
211 the glovebox, the sample carrousel was transferred in a custom, sealed, automatic sampler
212 pre-flushed with He. This automatic sampler was then reconnected to the EA and evacuated
213 for c.a. 20 min before opening it to the reduction column. This procedure suppresses any
214 contact of samples with atmospheric moisture that could rapidly re-hydrate the samples and
215 was found to increase overall reproducibility of the [H_2O^+] and D/H measurements.
216 Samples were combusted on an EA glassy carbon reaction tube, packed with glassy
217 carbon chips and enclosed in a ceramic liner to reduce hydroxyls to H_2. The temperature of
218 the column was kept at 1450°C by a Kanthal-Superthal heating element. High temperature
219 was required to ensure rapid sample reduction, to prevent CH_3 formation (Burgoyne and
220 Hayes, 1998) and to improve the reproducibility as already noticed by other authors (Sharp et
221 al., 2001; Gehre and Strauch, 2003). He carrier pressure was maintained at 120 kPa and the
222 produced gases were separated on a chromatographic column kept at 60°C. After
223 chromatographic separation, H_2 was introduced in the MS source through an open-split and
224 analyzed for D/H isotopic composition. H^{3+} correction was performed for each sample from

in house H_2 standard injections covering the sample signal range. The source trap current was kept at 500 mA and the samples were measured with a major peak height between 6 and 10 nA. The amount of H_2 produced was determined by comparing the major peak area with the signal produced during the analysis of internal standards.

Three different internal standards (Muscovite: MuscD65, Phlogopite: Mica-Mg and a fine grained marine sediment from the bay of Bengal: SO188) were routinely included during sample analysis to account for instrumental drift. These internal standards were calibrated against IAEA reference material NBS30 (Biotite, δD = -65.7 ‰), NBS22 (Oil, δD = -120 ‰) and CH-7 (Polyethylene, δD = -100.3 ‰) for D/H isotopic composition and MS linearity. $[H_2O^+]$ of the internal standards were calibrated against analysis of the same internal standards degassed using the same procedure on a classical extraction line involving extraction of water and subsequent reduction on a uranium furnace (Biegelsen et al., 1952). D/H is reported as δD and is normalized against SMOW. The overall, long term, 1 σ, reproducibility of the method on sediments and rocks is generally better than 2 ‰ for δD similar to the reproducibility obtained by Sharp et al., (2001) or Garzione et al., (2008) and 0.1 % for $[H_2O^+]$ (Figure A1, Appendix A). Samples were analyzed as duplicates.

4. RESULTS

The detailed composition of sediments used in this work is reported in the supplementary data file, table S1.

4.1 Mineral sorting and weathering systematic

The vertical depth profiles retrieved from rivers of the Ganga basin show a strong heterogeneity of the chemical composition of suspended sediments within the water column (Figure 2). Heterogeneities in river sediment chemistry as a function of sampling depth have been previously described for the Ganga-Brahmaputra and other large river (e.g. Galy et al., 2007; Bouchez et al., 2011a; 2011b; Garzanti et al., 2011; Lupker et al., 2011). The hydrodynamic control on the chemical composition of sediments in the Ganga River has been detailed in Lupker et al., 2011 and linked to mineral sorting effects (Garzanti et al., 2011). Briefly, the river hydrodynamical conditions of the sampled water column control the suspension of sediments based on their grain size, shape and density. For poly-mineralogical sediments, this results in a mineralogical and thus chemical differentiation of sediments within the water column.

The dominant minerals controlling the distribution of major elements in the water column are summarized in Table 1. Ganga sediment mineralogy is dominated by quartz, mica and feldspar, with occurrence of other phylosilicates, clay assemblages and hydroxides in the finer fraction. Calcite and dolomite are also abundant. For detailed mineralogical analysis see Garzanti et al. (2010) and Garzanti et al. (2011). In the Ganga River basin, sediment load increases bottomward by a factor of 2 to 3 between the shallowest and deepest samples. As illustrated in Figure 2, the major element composition of suspended sediments is variable from surface to bottom. SiO_2 concentration increases bottomward from 50 - 60 wt% in surface samples to 60 - 75 wt% for the deepest suspended sediments and up to 85 wt% in bedload samples. Na_2O concentrations in surface sediments also generally increase from surface (ca. 0.9 wt%) to bottom (ca. 1.1 to 1.3 wt%) for Himalaya front Rivers while Ganga sediments in Bangladesh have typical concentrations between ca. 1.0 and 1.2 wt%. On the contrary, Al_2O_3, Fe_2O_3, K_2O and H_2O^+ show decreasing concentrations bottomward. Al_2O_3 concentrations range from ca. 15 - 18 wt% in surface samples to ca. 10 - 14 wt% for the

deepest samples and down to 7 - 8 wt% in bedload samples. Fe_2O_3 concentrations range from 6 - 8 wt% in surface samples to 4 to 6 wt% in the deepest samples down to 2 - 3 wt% in the bedload. K_2O concentrations of typical surface sediments are of the order of 3 - 4 wt% and decrease to 2 - 3 wt% in deep sediments and 1 - 2 wt% in bedload samples. H_2O^+ concentrations range from ca. 3 - 4 wt% in surface samples to 1 - 2 wt% in deeper samples and down to 0.5 wt% in bedload samples. The D/H isotopic composition of sediments ranges from - 70 to - 110 ‰ and is not clearly dependant on sampling depth. Dolomite and calcite content of sediments is also highly variable depending on tributaries (from 0 to over 20 wt%) and shows no clear dependence with depth. As CaO and MgO contents reflect both carbonate and silicate detrital sources, the concentrations of CaO and MgO show a poor dependence with depth.

The large variability of sediment composition found in a single water column has to be accounted for to derive reliable information on the downstream evolution of the sediments during their transfer in the Gangetic floodplain. Following Galy and France-Lanord (2001) and in order to disentangle mineralogical sorting signals from the true chemical downstream evolution of sediments in large rivers, major elements were first normalized to silicon content to exclude dilution effects. Various elemental ratios of sediments are then evaluated with respect to their Al/Si molar ratio. Al/Si is used as a proxy of mineral sorting effects and is strongly correlated to grain size (Lupker et al., 2011). Coarse-grained sediments are enriched in quartz and have thus a low Al/Si ratio while finer grained surface sediments tend to be enriched in phylosilicates and clay minerals that have higher Al/Si ratios. The water column is thus well described by a range of Al/Si ratios and hydrodynamic mineral sorting results in a binary mixing trend between two end-members characterized respectively by a low Al/Si (coarse grained) and a high Al/Si (fine grained) ratio (Figure 3a). In the Himalayan system,

dissolved Si and Al represents only respectively ca. 1 % and less than 0.1 % of the particulate flux (Galy and France-Lanord, 2001). These elements can therefore be treated, to a first approximation, as immobile. Chemical weathering therefore results in the loss of the most mobile elements such as Na, K, Mg, Ca or a gain in hydration at constant Al/Si for steady state weathering. Hence, when considering samples collected along depth profiles, weathering is marked by a decrease (increase for H_2O^+/Si) in the slope of the linear relationship between mobile elements normalized to Si and Al/Si (Figure 3a). The chemical composition of the exported sediment flux may further influenced by sediment sequestration in the floodplain. Floodplain deposits tend to be enriched in coarse-grained and quartz-rich fractions. Conversely, the remaining transported load gets enriched in finer, clay rich sediments. This sequestration results in an apparent increase of the average Al/Si ratio of the transported sediments during floodplain transfer (Figure 3b). For the Ganga floodplain this effect remains however limited as only ca. 10 % of the transported load is deposited in the floodplain thereby increasing the average Al/Si ratio of the transported load from 0.22 at the Himalayan front to 0.23 for the Ganga in Bangladesh (Lupker et al., 2011). The weathering of Himalayan sediments can therefore be estimated by comparing the average chemical composition of river sediments sampled at different locations in the floodplain.

4.2. Spatial and temporal variation in chemical composition

4.2.1. Major elements

In this work we mainly focus on variability of the Fe/Si (Figure 4), Na/Si (Figure 5), K/Si (Figure 6), H_2O^+/Si (Figure 7) with respect to Al/Si ratio. All elements, but Na, show a systematic positive correlation with Al/Si showing the enrichment of the finer fraction (high

Al/Si) in Fe, K and H_2O^+ with respect to Si and the predominance of quartz in the coarser fraction (lower Al/Si ratio) as stated earlier. These correlations are linear for Fe, K and H_2O^+ suggesting a simple binary mixing between the coarse and fine-grained end-member. For Na the relationship is more complex and suggests a mixing between more than 2 end-members. These different end-members may be induced by mineralogical sorting of different minerals bearing Na such as albite (Garzanti et al., 2010; 2011) or due to the heterogeneity in the composition of the eroded lithologies (c.f. section 5.1.1). When considering each river individually, this relationship can be reasonably approximated by a log relationship for intermediate Al/Si ratios (0.15 – 0.30). The overall variability amongst rivers is higher for the finer fraction than for the coarse fraction. Bed-load sediments show a uniform average composition across the Gangetic plain even if some variability is observed. This second order variability can be mainly attributed to placer effects and accessory minerals. For each sampling year and location, the chemical composition of the sediments shows a unique mixing trend between an invariant bedload end-member and a variable fine-grained end-member. We will further describe the variability amongst rivers and sampling dates based on these correlations.

The major trans-Himalayan Rivers (the Yamuna, Ganga, Karnali, Narayani and Kosi) sampled at the Himalayan front (Himalayan front Rivers in Figure 4, 5, 6 and 7) show a comparable Fe/Si (Figure 4.a) and K/Si (Figure 6.a.) relationship with Al/Si. The Na/Si (Figure 5.a) and H_2O^+/Si (Figure 7.a) composition of these rivers shows more variability with a quasi-identical composition for the Yamuna, Ganga, Narayani and Kosi but a significant depletion in Na and enrichment in H_2O^+ for the Karnali sediments compared to the other trans-Himalayan Rivers.

After transiting in the floodplain and before merging with the Ganga mainstream the sediments from Himalayan Rivers (Himalayan floodplain Rivers in Figure 4, 5, 6 and 7) are

marked by a small but significant increase in Fe/Si ratios. Furthermore, these sediments also lose Na and K while they gain H_2O^+ during their course in the Gangetic floodplain. The relative loss is higher for Na than for K. Sediments from the Ganga shows the largest loss of Na and gain of H_2O^+ relative to Si during floodplain transfer while sediments from the Karnali and Kosi Rivers display the smallest loss/gain.

The sediments from the Ganga in Bangladesh, after mixing of all tributaries feeding the mainstream, have on average slightly higher Fe/Si ratios than Himalayan sediments and are significantly depleted in Na, K and enriched in H_2O^+ compared to Himalayan tributaries. The chemical composition of sediments sampled during 6 different sampling years on the Ganga in Bangladesh reveal an inter-annual variability for all elements (Figure 4c, 5c, 6c, 7c). This variability was not detected for Himalayan front Rivers when two different sampling years were available. The variability in sediment composition of the Ganga shows that years with high Fe/Si ratios (e.g. 2005) are also marked by low Na/Si and K/Si ratio, suggesting a common origin for the observed variations.

In order to derive a purely Himalayan weathering budget from the river sediments across the floodplain it is necessary to correct for additional non Himalayan tributaries such as the main southern tributary, the Chambal. Sediments from the Chambal have a distinct chemical composition characterized by higher Fe/Si and H_2O^+/Si ratios along with lower Na/Si and K/Si ratios compared to other rivers in the basin. This Chambal “fingerprint” can be followed further downstream in the Yamuna after its confluence with the Chambal (in Kalpi, see Figure 1) where sediments have similar chemical characteristics as Chambal sediments and even in the Ganga in Varanasi (after the confluence of the Ganga with the Yamuna) where the chemical composition is intermediate between Himalayan derived sediments and Chambal sediments. Addition of Chambal sediments to Himalayan derived

sediments decreases the Na/Si and K/Si ratios and increases the H_2O^+/Si ratio at the outlet and should not be attributed to chemical weathering in the floodplain.

Additionally, smaller tributaries draining the Siwaliks were also included in this work as they represent a potential additional source of sediments to the floodplain that is not captured by the trans-Himalayan Rivers sampled at the Himalayan front. Siwalik Rivers show a strong depletion in Na, a high H_2O^+ content and slightly higher Fe content than the other Himalayan Rivers. K on the contrary is similar to other Himalayan Rivers.

Finally the Gomti River represents a pure floodplain end member that is more depleted in Na, K and enriched in Fe and H_2O^+ than the Himalayan floodplain Rivers, showing the more weathered state of floodplain material.

4.3.3. D/H isotopic composition of sediments

The D/H isotopic composition (expressed as δD, ‰ V-SMOW) of the hydroxyls in the sediments from the Ganga basin is not strongly correlated to their degree of hydration (Figure 8). However, a shift towards less depleted, higher H_2O^+/Al ratios from the Himalayan front to the Ganga in Bangladesh is obvious. The field of the main hydrated primary minerals, *i.e.* muscovite and biotite have been determined from mono-mineralogical samples from extracted sediments in the Ganga basin (data in supplementary data file, table S2) and are compatible with the previously published analyses on Himalayan source rock minerals (France-Lanord et al., 1988a).

The composition of river sediment D/H composition can be explained by a mixing of muscovite and biotite more or less diluted by other aluminosilicates such as feldspar. The analyses of the clay fraction of samples from the Narayani at the Himalayan front and from the Ganga in Bangladesh (Figure 8) as well as the analysis of vermiculite minerals extracted

399 from Ganga sediments suggests however that secondary minerals are also significant
400 contributors to the H_2O^+ budget of the samples. The difference in isotopic composition
401 between these clay fractions is at least partly inherited from the difference in the isotopic
402 composition of surface waters in the High Himalayan range and the Gangetic floodplain
403 (respectively ca. – 50 to -135 ‰ and - 20 to - 65 ‰ as determined from river waters by
404 Gajurel et al., 2006). The increase in neo-formation of clay minerals during floodplain
405 transfer is consistent with the change in D/H isotopic composition of the sediments even if a
406 contribution of Chambal derived sediments must also be considered.
407
408 *4.3.4. Carbonates content and isotopic composition*
409
410 Himalayan Rivers and Ganga tributaries are characterized by a large variability in
411 carbonate content (Figure 9). The variability amongst Himalayan basins primarily reflects the
412 regional distribution of carbonated rocks. In Himalayan Rivers, carbonate dissolution during
413 floodplain transit is significant and highly variable amongst rivers (0 to 77 % loss for calcite
414 and 30 to 86 % loss for dolomite). This variability may derive from source effects and/or
415 temporal variations as Himalayan Rivers were not sampled simultaneously. Overall sediments
416 from the Ganga in Bangladesh have low carbonate content compared to sediments from its
417 upstream tributaries with ca. 3% calcite and 2% dolomite (Figure 9).
418
419 The isotopic composition of carbonates is shown in Figure 10 and is in agreement with
420 published data for bedload samples from the Ganga basin (Galy et al., 1999). In addition, the
421 composition of carbonates from Himalayan front Rivers fall within the field of carbonates
422 from Himalayan rocks (France-Lanord, 1987; Galy et al., 1999) supporting their detrital
423 origin. Calcite from Himalayan front Rivers sediments is characterized by a limited range in

$\delta^{18}O$ (from ca. -9 to -14 ‰) compared to all available data, while $\delta^{13}C$ values covers the full range of analyzed river sediments in this study. During floodplain transfer these values are shifted towards heavier $\delta^{18}O$ and lighter $\delta^{13}C$ values. Dolomite isotopic composition of Himalayan front Rivers sediments does not show any significant downstream evolution during transfer in the floodplain.

Sediments from the Chambal and Siwaliks Rivers have markedly contrasted carbonate isotopic compositions. Carbonates from Chambal sediments are significantly enriched in ^{18}O relative to those from Ganga sediments. In Siwalik Rivers sediments, calcite and dolomite are mainly ^{13}C depleted, which is consistent with Siwalik bulk carbonate isotopic composition (Supplementary data file, table S3; Sanyal et al., 2005). Sediment from the Karnali sampled downstream of the MBT display rather depleted carbonate ^{13}C compositions whereas upstream of the MBT carbonates from Karnali sediments are similar to other Himalayan Rivers sediments. Both calcite and dolomite from Ganga sediments in Bangladesh display $\delta^{13}C$ compositions that are compatible with a mixing of sediments from different Himalayan front Rivers. However, the higher $\delta^{18}O$ values, mainly for calcite, imply the contribution of another source of carbonates, such as Chambal carbonates, pedogenic carbonates from the Gangetic floodplain (Sinha et al., 2006) or biogenic shell carbonates (Gajurel et al., 2006).

4.3.5. Mg^s and Ca^s

As Mg and Ca concentrations are controlled by both carbonates and silicates, we calculated silicate derived Mg and Ca (noted Mg^s and Ca^s) correcting bulk concentrations for the contribution of carbonate minerals using the measured calcite and dolomite concentrations. Bulk calcium and magnesium concentrations were corrected based contributions of a pure calcite ($CaCO_3$) and dolomite ($Ca_{0.5}Mg_{0.5}CO_3$) component. On

449 average, carbonates account for 28% of the bulk sediment's Mg budget and 73% of the Ca
450 budget.

451 At the first order, calculated Mg^{s}/Si are positively and linearly correlated to Al/Si
452 ratios (r^2 > 0.75; Figure 11a). Scatter is nevertheless large and is most probably induced by
453 uncertainties associated with the dolomite correction. Himalayan front Rivers and Himalayan
454 floodplain Rivers are similar within the data scatter, while the Ganga in Bangladesh
455 consistently shows lower Mg^{s}/Si ratios than average Himalayan Rivers.

456 The calculated Ca^{s}/Si ratios span a relatively narrow range in spite of very variable
457 carbonate content (0 to 20 %). This strengthens our confidence in the carbonate correction,
458 because for such a variable carbonate content we would expect a higher range in the case of
459 an inaccurate correction. The calculated Ca^{s}/Si ratios show no correlation with Al/Si (Figure
460 11b). Within the Ganga basin, the Ca^{s}/Si ratio does not show a clear downstream evolution
461 during sediment transfer. The Ca^{s}/Si ratios of Himalayan Rivers sediments are overall very
462 low, which confirms that K, Na and Mg are the dominant silicate cations in the system (Galy
463 and France-Lanord, 1999).
464
465
466 **5. DISCUSSION**
467
468 **5.1. Source effects and temporal variability**
469
470 Sediments in the Ganga basin are characterized by both spatial and temporal
471 variability. To follow and quantify chemical weathering across the entire basin, it is necessary
472 to account for these variations. Inter-basin source effects and contributions from non
473 Himalayan sediments to the total sediment load of the Ganga have to be considered as they

would affect the overall sediment composition without being attributable to floodplain weathering.

5.1.1. Himalayan tributaries

With the exception of carbonates, the chemical composition of Himalayan front Rivers sediments is remarkably homogeneous. Given the contrasted Na/Si and H_2O^+/Si ratios of Himalayan source rocks from different units (Figure 12), this homogeneity suggests that the contribution of the different lithologic units is relatively uniform at the scale of the main Himalayan basins. The notable exception is the Karnali River whose sediments are characterized by lower Na/Si and higher H_2O^+/Si compared to sediments from other trans-Himalayan Rivers.

The unusual chemical composition of Karnali sediments could result from higher contributions of sediments from either the Lesser Himalaya or from the Siwalik. Upper Karnali and Behri Rivers sampled upstream of the Siwalik (sample # CA1004-6 and CA1001-3) show higher carbonate $\delta^{13}C$ values than downstream the Siwalik, which suggests a significant contribution of the Siwalik to the Lower Karnali River. Upper Karnali sediments have similar Na/Si ratios than sediments from other trans-Himalayan Rivers. In contrast Behri River sediments are depleted in Na, reflecting a high contribution of LH rocks. Bedload sediments from the Karnali at the Himalayan front also show very low Na/Si ratios, comparable to the Siwalik sediments, a signature that is not observed on the other trans-Himalayan Rivers. A crude mass balance based on the average Na/Si ratios (evaluated for an average Al/Si of 0.22) yields to ca. 25% Siwalik contribution to the total sediment load of the Karnali, assuming that the sediment flux of the Karnali is derived from a mixture of 1/3 of Upper Bheri and 2/3 of sediments equivalent to the Upper Karnali River sediments. Recycling

of Siwalik sediments in the Karnali basin was already suggested in a study using apatite fission track in modern sands (Van der Beek et al., 2006), and would be compatible with the high uplift and erosion rates documented during the Holocene for these frontal units (Lavé and Avouac, 2000; 2001).

The other trans-Himalayan Rivers drain less Siwaliks and no direct significant Siwalik contribution is observed in their sediments at the front of the Himalayan range. Based on He-Pb dating of zircons, Campbell et al. (2005) also excluded a significant Siwalik contribution to the Ganga. Additional significant contributions of second order rivers draining the southern flank of the Siwalik and contributing to the Ganga sediment load in the floodplain is also unlikely as the high subsidence and accommodation space available in the inter-fan regions of the floodplain would trap large proportions of the sediments transported by these low stream power rivers.

5.1.2. Southern tributaries

The distinct Fe/Si ratios of the Chambal sediments can be used to trace its contribution to the Ganga sediment load. The linear trend defined by Fe/Si and Al/Si ratios in Himalayan front Rivers is homogeneous and is only slightly affected during floodplain transfer (Figure 4). Specifically, Yamuna sediments at the Himalayan front have typical Himalayan compositions. But Yamuna sediments sampled downstream of the confluence with the Chambal are indistinguishable from Chambal sediments (Figure 4, 5, 6, 7) implying that only a minor proportion of the Himalayan Yamuna sediments delivered to the floodplain by the Yamuna River are actually transported through the floodplain, which may have prevailed over the last 120 kyrs (Sinha et al., 2009). This is also consistent with the present day extensive use of water resources in the Western Gangetic plain. Further downstream on the Ganga in

Varanasi, the contribution of Chambal sediments is still high. Using the Fe/Si vs. Al/Si relationships of the sediments and assuming a similar grain size distribution for all contributing rivers (similar average Al/Si), we estimate that the contribution of Chambal sediments accounts for ca. 40% of the sediment load in 2001 and 20% in 2008.

At the outflow of the Ganga in Bangladesh, the inter-annual variability of sediment composition exceeds the variability observed amongst Himalayan Rivers and can thus only be attributed to the contribution of sediments from the Chambal or other southern tributaries. In 2005, unusually high Fe/Si ratios combined with low Na/Si and K/Si ratios suggest a high proportion of Chambal sediments. Conversely, sediments sampled in 2004 are characterized by low Fe/Si ratios and hydration as well as high Na/Si and K/Si ratios. Based on the Al/Si vs Fe/Si regressions defined by sediments collected along depth profiles on the Ganga in Bangladesh it is possible to estimate the contribution of Chambal sediments to the Ganga sediment load. Using the Himalayan floodplain Rivers as a reference, this mass balance calculation shows that the Chambal contributes to up to 17% of the suspended load in Bangladesh in 2005 and ca. 4 % in 2007 and 2008. This estimate assumes that Ganga and Chambal sediments are characterized by a similar average Al/Si of 0.23 (Lupker et al., 2011). We note that the average Al/Si of the Chambal sediment load is not well constrained and that in the event this river mainly contributed to the finer load of the Ganga (i.e. with higher Al/Si) our mass balance calculation would overestimate the Chambal sediment contribution (Supplementary data file, table S4). In 2002, 2004 and 2010 the Fe/Si vs Al/Si trend defined by Ganga sediments is incompatible with mixing between Himalayan floodplain Rivers sediments and Chambal sediments, which excludes a significant Chambal input and points towards second order source effects within the catchments. The contribution of Chambal sediments to the whole Ganga sediment load was also estimated at ca. 5 % based on their

548 relative Sr, Nd and Os isotopic signatures (Singh et al., 2008; Paul, 2008), but these studies do
549 not account for any temporal variability.
550 Variable proportions of Chambal sediments must be accounted for when considering
551 the fate of Himalayan sediments in the system as the composition of Chambal sediments in
552 Na, K and H_2O^+ is very distinct from that of Himalayan sediments. Inter-annual variability of
553 Chambal sediment contribution to the Ganga sediment load also highlights that even in these
554 large systems, the transfer of suspended sediments can be rapid and vary on an annual basis.
555 In spite of its large scale, the Ganga system is thus not fully buffered regarding high
556 frequency variations in its input.
557
558 **5.2. Locus of continental weathering**
559
560 *5.2.1. Quantifying weathering intensity from river sediments*
561
562 To quantitatively assess the role of the Gangetic floodplain in chemical weathering of
563 Himalayan sediments we attempt to characterize and quantify chemical weathering from
564 source to sink. For a given grain size class *i*, the loss or gain in mobile elements *X* normalized
565 to Si ($\Delta {}^{X}\!/_{Si}|^{i}$) can be derived from the difference of composition between upstream and
566 downstream river sediments following eq. (1a):

567 $$\Delta {}^{X}\!/_{Si}{}^{i} = \left({}^{X}\!/_{Si}|^{i}_{upstream} - {}^{X}\!/_{Si}|^{i}_{downstream} \right) \quad (1a)$$

568 because grain-size is strongly correlated to the chemical composition and especially to the
569 Al/Si ratio of sediments (Bouchez et al., 2011b; Lupker et al., 2011), equation (1a) can be
570 rewritten as equation (1b):

571 $$\Delta {}^{X}\!/_{Si}{}^{Al/Si} = \left({}^{X}\!/_{Si}|^{Al/Si}_{upstream} - {}^{X}\!/_{Si}|^{Al/Si}_{downstream} \right) \quad (1b)$$

572 Finally, the average loss of mobile elements ($\Delta\overline{X/Si}$) for a given river reach can be determined
573 at the first order, provided that the average Al/Si of the transported sediments is known:

574 $$\Delta\overline{X/Si} = \left(\overline{X/Si}\Big|_{upstream} - \overline{X/Si}\Big|_{downstream}\right) \quad (1c)$$

575 A change in Si concentration during floodplain transfer can occur because of Si dissolution
576 and sequestration of Si-rich material in the floodplain. The dissolved silicon flux in the
577 Himalayan system accounts for only ca. 1% of particulate silicon flux (Galy and France-
578 Lanord, 2001). Furthermore, Lupker et al. (2011) estimated that about 10 % of the Himalayan
579 sediment flux is stored in the floodplain in the form of low Al/Si material. A simple mass
580 balance calculation using the Si content of sediments exported by the Ganga in Bangladesh
581 and the Si content of Ganga bedload as analogue for floodplain material (Lupker et al., 2011)
582 shows that the decrease in Si concentration due to sequestration is limited to less than 2 % of
583 the initial Si content. These two effects are therefore neglected as they remain within the
584 overall uncertainty of the method. The changes in absolute elemental concentrations can thus
585 be approximated to a first order by changes in the silicon-normalized concentrations.

586

587 Based on the sample set presented in this work it is possible to partition the loss of
588 mobile elements between the losses occurring within the Himalayan range (2a), the northern
589 part of the floodplain (2b) and the southern part of the floodplain (2c):

590 $$\Delta\overline{X/Si}\Big|_{HimalayanRange} = \left(\overline{X/Si}\Big|_{HimalayanCrust} - \overline{X/Si}\Big|_{HimalayanFrontRivers}\right) \quad (2a)$$

591 $$\Delta\overline{X/Si}\Big|_{FloodplainN} = \left(\overline{X/Si}\Big|_{HimalayanFrontRivers} - \overline{X/Si}\Big|_{HimalayanFloodplainRivers}\right) \quad (2b)$$

592 $$\Delta\overline{X/Si}\Big|_{FloodplainS} = \left(\overline{X/Si}\Big|_{HimalayanFloodplainRivers} - \overline{X/Si}\Big|_{GangaBangladesh}\right) \quad (2c)$$

593

The Himalayan crust composition ($\overline{X/Si}\big|_{HimalayanCrust}$) is determined from an extensive bedrock sample data set (Galy and France-Lanord, 2001) that we further corrected to include Siwalik sediments (Supplementary data file, Table S6). These estimates only include Na, K and H_2O^+ as for the other elements the unknown distribution and initial content of carbonates in the Himalayan source rocks hampers meaningful estimates. In the floodplain, $\overline{X/Si}\big|_{HimalayanFrontRivers}$, $\overline{X/Si}\big|_{HimalayanFloodplainRivers}$ and $\overline{X/Si}\big|_{GangaBangladesh}$ are determined from averaging $\overline{X/Si}\big|_i$ of each river, *i*, of the considered reach. $\overline{X/Si}\big|_i$ is obtained using the relationship between X/Si and Al/Si and the average Al/Si of the sediments. For calcite and dolomite the average compositions are obtained by averaging the carbonate content of all samples available for each river as no correlation with Al/Si is observed. Details of the calculation can be found in Appendix B.

5.2.2. Floodplain weathering

The evolution of the X/Si ratio in the floodplain is represented in Figure 13. The resulting depletion in mobile elements calculated using equation (2) is given in Table 2. This depletion is computed for Al/Si = 0.23 in the floodplain (c.f. Appendix B). During floodplain transfer from the Himalayan front to the Ganga in Bangladesh sediments mainly loose Na, K and carbonates and gain H_2O^+ relative to silicon even if uncertainties remain high (Figure 13). The loss of Mg^s is limited and bears high uncertainties. For Ca^s, no significant change is observed considering the large uncertainties on average concentrations (Figure 11). Figure 13, shows that for each mole of Na lost in the floodplain, ca. 0.8 mole of K, 0.3 mole of Mg^s, and 2 to 3 moles of calcite and dolomite are lost while 1.4 moles of H_2O^+ are gained. Silicate weathering in the Gangetic floodplain mainly releases Na and K, a conclusion already

attained by dissolved load studies in the system (Sarin et al., 1989; Galy and France-Lanord, 1999; Huh, 2010). The absolute K content of Himalayan sediments is ca. 1.5 to 2 times higher than the Na content and the limited loss of K compared to Na therefore highlights the limited mobility of K. Compared to other silicate bound cations, the gain in H_2O^+ is very significant, which makes it a very sensitive proxy for silicate weathering.

As far as our data set is representative, Na and carbonates are preferentially lost and hydration preferentially gained in the Northern part of the floodplain, between the Himalayan front and the confluence with Ganga mainstream. On average, 70 % of the Na, 60 % of the calcite, 80 % of the dolomite depletion and almost 100 % of H_2O^+ gain in the floodplain is observed between the Himalayan front and the Ganga at Harding Bridge has occurred in the first part of the floodplain, which represents, however only ca. 25 % of the total floodplain area drained by the Ganga. K loss is more uniform across the floodplain. This weathering budget of the Himalayan Rivers shows that even a limited floodplain transfer distance (from ca. 590 km for the Ganga and Karnali; 375 km for the Narayani to 200 km for the Kosi) is sufficient to produce a significant weathering signal. This is especially striking in the case of the Narayani River whose floodplain drainage is very limited (ca. 7500 km^2) and does not collect significant sediments from lateral tributaries of the adjacent floodplain or Siwaliks. Using U-series disequilibria, Chabaux et al., 2006 and Granet et al., 2007 estimated that the average transfer time of coarse sediments between the Himalayan front and the confluence with the Ganga eaches up to 100 kyrs for the Karnali and Narayani although fine grain sediments are transferred in less than 25 kyrs (Granet et al., 2010). Long transfer times imply complex interactions exist between the sediments stored in the floodplain and modern river sediments (e.g. Meade et al., 1985; Dunne et al., 1998). Our data suggest that the floodplain / river interactions is a major control of the chemical composition of river

643 sediments. For a similar sediment flux, the upland distributed channels offer a higher active
644 floodplain to river channel ratio promoting exchange between both compartments. The Ganga
645 mainstream on the contrary is bound to a narrower floodplain in the south of the Gangetic
646 plain, which limits interactions. We however emphasize that even if the overall weathering
647 effect of the floodplain on Himalayan sediments is significant, large uncertainties and
648 potential temporal variability may bias our weathering estimates within the floodplain. These
649 caveats should be kept in mind when confronting these results to other studies.
650
651 Gomti River sediments provide a pure floodplain signal as the Gomti River is
652 currently disconnected from any direct Himalayan input (Singh et al., 2005). It cannot be
653 excluded that Gomti sediments originated from "Karnali like" sediments, already depleted in
654 Na. In any case, this river drains alluvial sediments that have experienced weathering for up
655 to 50 kyr (Srivastava et al., 2003). Gomti sediments are depleted in Na compared to Ganga
656 sediments in Bangladesh (Figure 13). But comparatively, K depletion and H_2O^+ gain is
657 limited while Mg^s and Ca^s content is similar to that of Ganga sediments in Bangladesh (Figure
658 10). This is consistent with 1) higher mobility of Na compared to K during floodplain
659 weathering in the Ganga system and 2) the limited loss of silicate Mg and Ca by Himalayan
660 sediments even during very prolonged weathering in the floodplain.
661
662 *5.2.3. Comparison with Himalayan weathering*
663
664 The chemical weathering that occurs in the Gangetic floodplain (section 5.2.2.) can be
665 compared to the weathering of sediments that occurs within the Himalayan range. The latest
666 was determined from equation (2a) for Na, K and H_2O^+ using the composition of Himalayan
667 front Rivers sediments evaluated for Al/Si = 0.22 and the Himalayan crust (Figure 13). This

668 comparison, solely based on the chemical composition of the solid phase in the system shows
669 that 1) Na is mainly lost in the floodplain where ca. 60 % of the total Na loss of the
670 Himalayan system occurs, 2) the loss of K and gain of hydration recorded by the sampled
671 sediments significantly occurs in the floodplain but does not appear significant in the
672 Himalayan range. For K, the apparent loss in the Himalayan range is negligeable. France-
673 Lanord et al. (2003) however show that the dissolved flux of K in the Himalayan front rivers
674 is significant. This highlights that the Himalayan crust composition we use may not be fully
675 representative of the eroded material or that uncertainties are to high to detect a loss of K and
676 gain in H_2O^+. Nevertheless it also suggests that K weathering and hydration in the Himalayan
677 range remains limited while it is significant and resolvable in the floodplain.
678 By using the river sediment composition we show that chemical weathering in the
679 Gangetic floodplain most probably dominates the weathering in the Himalayan range, which
680 is consistent with the conclusions reached by studies of dissolved species in the Himalayan
681 system (Galy and France-Lanord, 1999; West et al., 2002). However, our conclusion relies on
682 the accuracy of the average composition of the eroded Himalayan crust. Evaluating the
683 composition of the Himalayan crust remains a challenging task and is sensitive to sampling
684 biases. Refining the weathering budget from detrital sediments thus requires a better
685 constrains on source rocks composition as already underlined by Gaillardet et al. (1999b).
686
687 *5.2.4. Possible weathering mechanisms*
688
689 Although the purpose of this study is not to determine the exact weathering reactions
690 occurring in the floodplain, the systematic release of Na, K and uptake of OH allow
691 speculating about the possible reactions occurring in the floodplain. Albite being the main Na

carrier in Ganga sediments (Garzanti et al., 2011), the release of Na is mainly attributed to its weathering into kaolinite or smectite.

K-feldspar dissolution likely represents a source of K. Additionally, abundant vermiculite in floodplain river sediments also supports biotite weathering. The molar K/Mg ratio of Himalayan biotites is ca. 1 (eg. Garzanti et al., 2011; Supplementary data file, Table S7) but during weathering into vermiculites, biotites preferentially loose K, while Mg is immobile or readsorbed as hydrated ion (Velde and Meunier, 2008). This mechanism is supported by semi quantitative SEM-BSE analyses of hand picked biotites and vermiculites showing that K/Al decreases and Mg/Al increases during vermiculitisation (Supplementary data file, Table S7). Muscovite is generally more stable than biotite (e.g. Wilson, 2004) but may also contribute to the dissolved K flux.

Increase in hydration is particularly high during clay and hydroxides formation, which is most favorable during longer transfer times in a wet and warm environment such as the Gangetic plain. Tomar (1987), Sarin et al. (1989) and more recently Heroy et al. (2003) and Huyghe et al. (2010), showed the increasing proportion of smectites and other expandable clays over illite from the Himalayan front Rivers to the floodplain Rivers further downstream. This increase in the proportion of secondary minerals in the floodplain is confirmed by both the elemental (H_2O^+/Al) and isotopic (δD) composition of the sediments (Figure 8). Increasing δD values and H_2O^+/Al ratios of the sediments during floodplain transfer reflect the incorporation of a larger proportion of clay minerals in equilibrium with floodplain surface waters, as revealed by the composition of < 2 µm fractions. H_2O^+/Al and δD of detrital sediments are thus indicative of the location of secondary mineral formation.

Concerning carbonates, the dissolution rates of calcite and dolomite are surprisingly equivalent. During laboratory experiments, calcite was found to dissolves 5 to 10 times faster than dolomite (eg. Morse and Arvidson, 2002; Prokovsky et al., 2005; Yadav et al., 2008).

717 Szramek et al., 2007 showed, however, using solute chemistry in temperate rivers that the
718 calcite/dolomite dissolution ratio in carbonate bearing watershed reaches 0.6 to 0.7. It has
719 been shown that the Ganga and its tributaries are supersaturated with respect to calcite at least
720 during lean flow (Sarin et al., 1989; Galy and France-Lanord, 1999; Dalai et al., 2002;
721 Jacobson et al., 2002). High dissolved Ca^{2+} concentrations are therefore suspected to hamper
722 calcite dissolution in the floodplain.
723
724 The chemical budgets derived in this work also highlight the different behavior of Na
725 and K. While Na weathering is significant in both the Himalayan range and the Gangetic
726 floodplain, K weathering predominantly occurs in the floodplain. This behavior can be
727 interpreted in the light of the specific weathering rates of the main Na and K bearing minerals,
728 *i.e.* albite and biotite respectively. As Hilley et al., (2010) recently pointed out, the theoretical
729 behavior of minerals with respect to weathering in an erosive context is highly variable and
730 depends on specific weathering rates of each mineral. While considering Himalayan physical
731 erosion rates albite is weathered in supply-limited regime, biotite remains in reaction-limited
732 regime. In the floodplain, lower physical erosion rates or longer residence times (Granet et al.,
733 2010) favor supply-limited regime and high chemical weathering rates for both minerals.
734 These inferences should nevertheless be confirmed by dedicated mineralogical observations.
735
736 **5.3. Floodplain weathering budget**
737
738 The flux of elements weathered in the floodplain and delivered to the dissolved load
739 ($\varphi_X|_{Floodplain}$) is the sum of the flux of elements lost by the sediments during their transfer in
740 the floodplain ($\varphi_X|_{RiverSediments}$) and by the sediments stored in the floodplain ($\varphi_X|_{StoredSediments}$):
741 $$\varphi_X|_{Floodplain} = \varphi_X|_{RiverSediments} + \varphi_X|_{StoredSediments} \quad (3)$$

742 Reliably assessing the weathering flux associated with the sediments stored in the floodplain
743 remains difficult. The extent of weathering reactions occurring within the sediment column of
744 the floodplain is largely unknown. Furthermore the timescale involved for weathering stored
745 sediments or river sediments is most probably different, which hampers a correct quantitative
746 comparison of both fluxes. However on a qualitative basis this flux remains most probably
747 limited. Floodplain sequestration is limited to ca. 10 % of the Himalayan flux and the average
748 Al/Si of the stored material is low at ca. 0.17 (Lupker et al., 2011). The river sediment data of
749 this work suggests that the loss of mobile elements at lower Al/Si ratios is limited. We
750 therefore suggest here that $\varphi_X|_{RiverSediments} > \varphi_X|_{StoredSediments}$. The floodplain budget presented
751 here is therefore limited to the loss of mobile elements of the sediment load effectively
752 exported by the Ganga basin and may slightly underestimate the complete weathering budget
753 of the floodplain.
754
755 The chemical weathering intensity derived in section 5.2 can therefore be used to
756 estimate the weathering flux of the Gangetic floodplain. Using an average sediment flux (F_{sed})
757 of the Ganga of ca. 400 to 500 Mt/yr (RSP, 1996; Lupker et al., 2011) and an average Si
758 content of Ganga sediments ($\overline{[Si]}$) of ca. 10.6 mol/kg (Lupker et al., 2011) it is possible to
759 estimate the flux of elements transferred from the particulate to the dissolved load during
760 chemical weathering in the floodplain following equation (3):
761 $$\varphi_X|_{Floodplain} = F_{sed} \cdot \overline{[Si]} \cdot \left(\Delta \overline{X/Si}|_{FloodplainS} + \Delta \overline{X/Si}|_{FloodplainN} \right) \quad (4)$$
762 Results computed with equation (4) are reported in Table 3. Carbonate Ca and Mg are the
763 main cations released to the dissolved load. Na release is 30 % higher than that of K while
764 Mg^s dissolution flux is limited to less than $20 \cdot 10^9$ moles/yr. Ca^s dissolution flux could not be
765 determined accurately due to the high heterogeneity of sediment composition. But, owing to

766 the lack of significant change and the overall low Ca^s/Si ratios, Ca^s losses can be considered
767 small (< $10 \cdot 10^9$ moles/yr). These estimates show that weathering can be quantitatively derived
768 from the study of detrital sediments transported by rivers even if calculated fluxes rely on the
769 accurate determination of both total sediment flux and average chemical composition and bear
770 high uncertainties.

771 The weathering fluxes computed from the river sediments in the Ganga plain were
772 compared to the total dissolved fluxes exported out of the basin (Table 3). The dissolved
773 fluxes of the Ganga are taken from Galy and France-Lanord (1999) and corrected for cyclic
774 input. This comparison shows that the weathering fluxes computed in this work are on the
775 same order as total dissolved fluxes currently exported out of the basin. Even if large
776 uncertainties are bound to both estimates this highlights the conclusion drawn above that
777 weathering in the floodplain is significant and probably exceeds weathering in the Himalayan
778 range.

779

780 It should however be noted that $\varphi_X|_{Floodplain}$ deduced from equation (4) only accurately
781 represents the modern weathering flux generated in the floodplain under the assumption that
782 weathering proceeds at steady state. Equation (4) assumes that F_{sed} is constant over the time
783 scale of sediment residence time in the floodplain. Furthermore, any transient change in soil
784 formation/erosion in the floodplain on the time scale of sediment transfer time will lead to an
785 additional sink/source of fine grained sediments within the floodplain that may not have been
786 accounted for and hence may bias $\varphi_X|_{Floodplain}$. This latest has been previously suggested for
787 the Amazon basin, with a recent increase in the export of mature sediments from the
788 floodplain (Gaillardet et al., 1999; Bouchez et al., 2011c) and should be assessed for the
789 Ganga basin in the near future. These limitations should therefore be kept in mind when
790 comparing these weathering fluxes to other estimates such as the dissolved load.

6. CONCLUSIONS

Studying the downstream evolution of the chemical composition of river sediments in the Ganga basin we show that sediments can be used as a quantitative tracer of chemical weathering. Sediment vertical depth profiles show that the chemical variability generated by mineral sorting within the water column exceeds the variability observed among all sampling locations and dates. A single sample is thus merely representative of the sediment flux and cannot be used *a priori* to derive global scale weathering budgets. Using relations between silicon-normalized mobile element concentrations with Al/Si ratios it is possible to derive an average chemical composition for a given river section. Using this approach, we followed the chemical composition of river sediments from the Himalayan front downstream to the Ganga in Bangladesh, across the whole Gangetic floodplain. By integrating the spatial variability among Himalayan tributaries and the temporal variability associated with variable inputs of southern tributaries such as the Chambal, we budget the loss of chemical elements by Himalayan sediments. This budget shows that sediments undergo a significant depletion in Na, K, Ca and Mg that is correlated to a gain in hydration during floodplain transfer. Carbonate dissolution dominates the loss of elements and accounts for respectively ca. $190 \cdot 10^9$ and $70 \cdot 10^9$ mol/yr of Ca and Mg released to the dissolved load. Silicate weathering in the floodplain mainly releases Na and K (ca. $50 \cdot 10^9$ and $40 \cdot 10^9$ mol/yr, respectively). By comparison, the loss of silicate Mg and Ca is limited to less than $20 \cdot 10^9$ and $10 \cdot 10^9$ mol/yr respectively. Weathering in the floodplain is thus significant, but only a limited amount of the produced alkalinity can be attributed to silicate Ca release. Hence, weathering of Himalayan sediments in the Gangetic floodplain is a relatively limited carbon sink, mainly owing to the low Ca silicate content of Himalayan source rocks. Furthermore we show that sediment

hydration is a sensitive weathering tracer that can be used in detrital settings, such as the Himalayan system. Comparison of the floodplain weathering budget with the weathering budget obtained by difference with the composition of the Himalayan crust, suggests that silicate weathering is predominantly occurring in the floodplain. However this comparison suffers from the difficulty to accurately assess the source rock composition, specifically for K. A comparison with total dissolved weathering fluxes of the Ganga supports this affirmation even if it should be reminded that these could only be compared under the assumption of steady-state weathering.

The chemical composition of river sediments contains a weathering signal that can be quantitatively used to study chemical weathering, provided that first order mineral sorting effects are taken into account. This conclusion supports the use of sedimentary records around the globe for paleo-weathering studies in order to document how surface processes were affected by major geological changes. This work also stresses the need to use a source to sink approach when considering weathering in earth surface systems as in large-scale basins, weathering may not be restricted to high uplift/erosion areas but can also be significantly occurring in the downstream, low land areas.

Acknowledgments:

We like to thank Estelle Blaes, Louis France-Lanord, Marion Garçon, and Britta Voss for their enthusiastic help with sampling. We are also indebted to D. Sparks, J. West and K. Huntington as well as an anonymous reviewer who provided thoughtful reviews and comments. This manuscript further benefited from fruitful discussions with Julien Bouchez and Albert Galy. This work was supported by INSU program “Relief de la Terre” and ANR Calimero. Valier Galy was supported by the U.S. National Science Fundation (Grant OCE-0851015).

APPENDIX A – [H_2O^+] AND δD REPRODUCTIBILITY

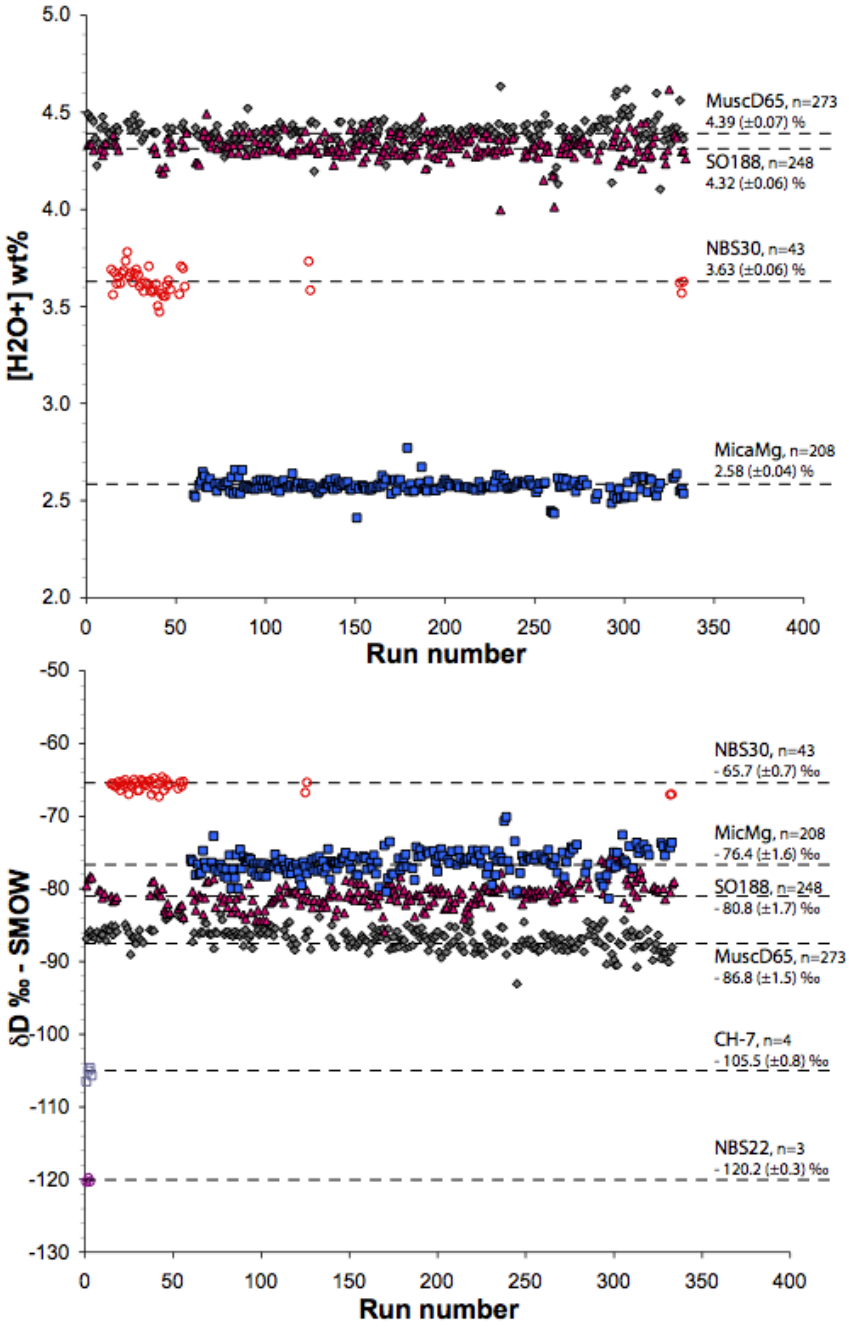

Figure A1: Replicate analysis of internal standards MuscD65, Mica-Mg and SO188 for H_2O^+ concentration (top figure) and D/H isotopic composition (lower figure) routinely measured. Measurements of international reference (NBS 30, NBS 22 and CH-7) are also indicated.

APPENDIX B – DETERMINATION OF AVERAGE HIMALAYAN CRUST AND SEDIMENT COMPOSITION

The Himalayan crust chemical composition used in this work is derived from the average composition of HHC and LH rocks as compiled by Galy and France-Lanord (2001), with the addition of samples from Pecher (1978) and Brouand (1987). The average Nd isotopic composition of Himalayan sediments indicates that ca. 80 % of sediments are derived from the HHC and 20 % from LH (Galy and France-Lanord, 2001). We further corrected this estimate for Siwalik contribution as the Siwalik represent a source of sediments to the Gangetic system that must be accounted for (see section 5.1.1.). Lavé and Avouac (2001) have estimated the relative contribution of Siwalik sediment to ca. 15 to 20 % of the total sediment flux. However, those fluxes are in large part deposited in the Ganga plain between the mega fans of the main transhimalayan Rivers, so that we arbitrarily estimated that only ca. 10 % of sediments transported by the floodplain Rivers are from Siwalik origin. Therefore $\overline{X/Si}\big|_{HimalayanCrust}$ is given by equation (B1):

$$\overline{X/Si}\big|_{HimalayanCrust} = 0.72 \cdot \overline{X/Si}\big|_{HHC} + 0.18 \cdot \overline{X/Si}\big|_{LH} + 0.10 \cdot \overline{X/Si}\big|_{Siwaliks} \quad \text{(B1)}$$

Uncertainties on source rock composition and on the relative proportions of each geological unit are propagated through the calculation (c.f. supplementary data, Table S6).

For the Himalayan front and floodplain river sediments, $\overline{X/Si}\big|_{HimalayanFrontRivers}$ and $\overline{X/Si}\big|_{HimalayanFloodplainRivers}$ are determined from chemical composition of each river of the reach, $\overline{X/Si}\big|_i$ (e.g. he Yamuna, Ganga, Karnali, Narayni and Kosi for the Himalayan front) weighted by its respective sediment flux, F_i:

$$\overline{X/Si}\big|_{HimalayanFrontRivers, HimalayaFloodplainRivers} = \frac{1}{\sum_i F_i} \cdot \sum_i F_i \cdot \overline{X/Si}\big|_i \quad \text{(B2)}$$

Fluxes are mainly derived from sediment gauging data (HMG, Nepal Electr. Author., 1982; Ghimire and Uprety, 1990; Sinha and Friend, 1994) or from cosmo-nuclides derived erosion rates (Vance et al., 2003). We conservatively propagated 50 % uncertainty on these fluxes. For the Ganga in Bangladesh, $\overline{X/Si}\big|_{GangaBangladesh}$ was determined from averaging each sampling year after correction for potential Chambal sediment contribution (as discussed in section 5.1.2):

$$\overline{X/Si}\big|_{GangaBangladesh} = \frac{1}{i} \cdot \sum_{i} \overline{X/Si_{corrected}}\big|_{i} \quad \text{(B3)}$$

For all river sediments, $\overline{X/Si}\big|_{i}$ was determined through the regression between, X/Si and Al/Si (linear for Fe, K, H_2O^+ and Mg^s and logarithmic for Na, c.f. Figure 4, 5, 6, 7 and 11) and the average Al/Si of the sediments. Because the chemical composition of bedload samples is affected by placer effects and because these bedload samples have a strong control on the regression between Al/Si and X/Si, we chose to force the regressions through a uniform bedload composition obtained after averaging all available bedloads in the Ganga floodplain. This is justified, as even if the bedload composition is variable between sampling sites or dates, there is no significant and systematic evolution in bedload composition in the floodplain. When considering Himalayan weathering, the averaged Al/Si used to determine $\overline{X/Si}\big|_{i}$ is 0.22 as this is the average Al/Si determined for the Himalayan crust and for Himalayan front River sediments (Lupker et al., 2011). When considering floodplain weathering, the average Al/Si used is 0.23 as the average material that is effectively transported through the entire Ganga floodplain has a ratio of 0.23 due due to sediment sequestration in the floodplain (Lupker et al., 2011). For calcite and dolomite content, $\overline{X/Si}\big|_{i}$ is obtained by averaging the composition of all available samples of a given river as no relation to Al/Si is found.

References

Attal, M. and Lave, J., 2006. Changes of bedload characteristics along the Marsyandi River (central Nepal): Implications for understanding hillslope sediment supply, sediment load evolution along fluvial networks, and denudation in active orogenic belts. In: Willett, S. D., Hovius, N., Brandon, M. T., and Fisher, D. M. Eds.), Tectonics, climate, and landscape evolution.

Berner, R., Lasaga, A., and Garrels, R., 1983. The carbonate-silicate geochemical cycle and its effect on atmospheric carbon dioxide over the past 100 million years. *Am. J. Sci* **283**, 641–683.

Berner, R. A., 1994. GEOCARB-II - A Revised Model of Atmospheric CO2 over Phanerozoic Time. *American Journal of Science* **294**, 56-91.

Bigeleisen, J. L., Perlman, M., and Prosser, H. C., 1952. Conversion of hydrogenic material to hydrogen for isotopic analyses. *Analytical Chemistry* **24**, 1356-1357.

Bouchez, J., Metivier, F., Lupker, M., Maurice, L., Perez, M., Gaillardet, J., and France-Lanord, C., 2011a. Prediction of depth-integrated fluxes of suspended sediment in the Amazon River: particle aggregation as a complicating factor. *Hydrological Processes* **25**, 778-794.

Bouchez, J., Gaillardet, J., France-Lanord, C., Maurice, L., and Dutra-Maia, P., 2011b. Grain size control of river suspended sediment geochemistry: Clues from Amazon River depth profiles. *Geochem. Geophys. Geosyst.* **12**, Q03008.

Bouchez, J., Lupker, M., Gaillardet, J., France-Lanord, C., and Maurice, L., 2011c. How important is it to integrate riverine suspended sediment chemical composition with depth? Clues from Amazon River depth-profiles. *Geochimica Et Cosmochimica Acta* **75**, 6955-6970.

Brouand, M., 1987. Pétrogenèse des migmatites de la dalle du tibet (Himalaya du Népal),

Insitut National Polytechnique de Lorraine (INPL) – Nancy, 366p.

Burgoyne, T. W. and Hayes, J. M., 1998. Quantitative Production of H2 by Pyrolysis of Gas Chromatographic Effluents. *Analytical Chemistry* **70**, 5136-5141.

Campbell, I. H., Reiners, P. W., Allen, C. M., Nicolescu, S., and Upadhyay, R., 2005. He–Pb double dating of detrital zircons from the Ganges and Indus Rivers: Implication for quantifying sediment recycling and provenance studies. *Earth and Planetary Science Letters*, 402-432.

Carignan, J., Hild, P., Mevelle, G., Morel, J., and Yeghicheyan, D., 2001. Routine analyses of trace elements in geological samples using flow injection and low pressure on-line liquid chromatography coupled to ICP-MS: A study of geochemical reference materials BR, DR-N, UB-N, AN-G and GH. *Geostandards Newsletter-the Journal of Geostandards and Geoanalysis* **25**, 187-198.

Chabaux, F., Granet, M., Pelt, E., France-Lanord, C., and Galy, V., 2006. U-238-U-234-Th-230 disequilibria and timescale of sedimentary transfers in rivers: Clues from the Gangetic plain rivers. *Journal of Geochemical Exploration* **88**, 373-375.

Dalai, T. K., Krishnaswami, S., and Sarin, M. M., 2002. Major ion chemistry in the headwaters of the Yamuna river system: : Chemical weathering, its temperature dependence and CO2 consumption in the Himalaya. *Geochimica Et Cosmochimica Acta* **66**, 3397-3416.

Donnadieu, Y., Goddéris, Y., Ramstein, G., Nédélec, A., and Meert, J., 2004. A ‘snowball Earth’climate triggered by continental break-up through changes in runoff. *Nature* **428**, 303-306.

Dunne, T., Mertes, L. A. K., Meade, R. H., Richey, J. E., and Forsberg, B. R., 1998. Exchanges of sediment between the flood plain and channel of the Amazon River in Brazil. *Geological Society of America Bulletin* **110**, 450-467.

946 Fasullo, J. and Webster, P. J., 2003. A hydrological definition of Indian monsoon onset and
947 withdrawal. *Journal of Climate* **16**, 3200-3211.
948 France-Lanord, C., 1987. Chevauchement, métamorphisme et magmatisme en Himalaya du
949 Népal central. Etude isotopique H, C, O. Thèse, Institut National Polytechnique de
950 Lorraine.
951 France-Lanord, C., Sheppard, S. M. F., and Le Fort, P., 1988. Hydrogen and oxygen isotope
952 variations in the High Himalaya peraluminous Manaslu leucogranite : evidence for
953 heterogeneous sedimentary sources. *Geochimica et Cosmochimica Acta* **52**, 513-526.
954 France-Lanord, C. and Derry, L. A., 1997. Organic carbon burial forcing of the carbon cycle
955 from Himalayan erosion. *Nature* **390**, 65-67.
956 France-Lanord, C., Evans, M., Hurtrez, J. E., and Riotte, J., 2003. Annual dissolved fluxes
957 from Central Nepal rivers: budget of chemical erosion in the Himalayas. *Comptes*
958 *Rendus Geoscience* **335**, 1131-1140.10.1016/j.crte.2003.09.014|ISSN 1631-0713
959 Gaillardet, J., Dupré, B., and Allègre, C. J., 1999. Geochemistry of large river suspended
960 sediments: silicate weathering or recycling tracer? *Geochimica Et Cosmochimica Acta*
961 **63**, 4037-4051.
962 Gaillardet, J., Dupré, B., Louvat, P., and Allègre, C. J., 1999. Global silicate weathering and
963 CO2 consumption rates deduced from the chemistry of large rivers. *Chemical Geology*
964 **159**, 3-30.
965 Gajurel, A. P., 1998. Géochimie isotopique et déformations synsédimentaires des dépôts du
966 bassin de Kathmandou. DEA, Université Joseph Fourier.
967 Galy, A. and France-Lanord, C., 1999. Weathering processes in the Ganges-Brahmaputra
968 basin and the riverine alkalinity budget. *Chemical Geology* **159**, 31-60.
969 Galy, A. and France-Lanord, C., 2001. Higher erosion rates in the Himalaya: Geochemical
970 constraints on riverine fluxes. *Geology* **29**, 23-26.

971 Galy, A., France-Lanord, C., and Derry, L. A., 1999. The strontium isotopic budget of
972 Himalayan Rivers in Nepal and Bangladesh. *Geochimica Et Cosmochimica Acta* **63**,
973 1905-1925.
974 Galy, V., France-Lanord, C., Beyssac, O., Faure, P., Kudrass, H., and Palhol, F., 2007.
975 Efficient organic carbon burial in the Bengal fan sustained by the Himalayan erosional
976 system. *Nature* **450**, 407-U6.
977 Galy, V., France-Lanord, C., and Lartiges, B., 2008. Loading and fate of particulate organic
978 carbon from the Himalaya to the Ganga-Brahmaputra delta. *Geochimica et*
979 *Cosmochimica Acta* **72**, 1767–1787.
980 Garzanti, E., Ando, S., France-Lanord, C., Censi, P., Vignola, P., Galy, V., and Lupker, M.,
981 2011. Mineralogical and chemical variability of fluvial sediments 2. Suspended-load
982 silt (Ganga-Brahmaputra, Bangladesh). *Earth and Planetary Science Letters* **302**, 107-
983 120.
984 Garzanti, E., Ando, S., France-Lanord, C., Vezzoli, G., Censi, P., Galy, V., and Najman, Y.,
985 2010. Mineralogical and chemical variability of fluvial sediments: 1. Bedload sand
986 (Ganga-Brahmaputra, Bangladesh). *Earth and Planetary Science Letters* **299**, 368-
987 381.
988 Garzione, C. N., Hoke, G. D., Libarkin, J. C., Withers, S., MacFadden, B., Eiler, J., Ghosh,
989 P., and Mulch, A., 2008. Rise of the Andes. *Science* **320**, 1304-1307.
990 Gehre, M. and Strauch, G., 2003. High-temperature elemental analysis and pyrolysis
991 techniques for stable isotope analysis. *Rapid Communications in Mass Spectrometry*
992 **17**, 1497-1503.
993 Ghimire, G. and Uprety, B., 1990. Causes and effects of siltation on the environment of
994 Nepal. *The Environmentalist* **10**, 55-65.
995 Gilg, H. A. and Sheppard, S. M. F., 1996. Hydrogen isotope fractionation between kaolinite

996 and water revisited. *Geochimica Et Cosmochimica Acta* **60**, 529-533.
997 Girard, J. P., Freyssinet, P., and Chazot, G., 2000. Unraveling climatic changes from
998 intraprofile variation in oxygen and hydrogen isotopic composition of goethite and
999 kaolinite in laterites: An integrated study from Yaou, French Guiana. *Geochimica Et*
1000 *Cosmochimica Acta* **64**, 409-426.
1001 Gislason, S. R., Oelkers, E. H., and Snorrason, A., 2006. Role of river-suspended material in
1002 the global carbon cycle. *Geology* **34**, 49-52.
1003 Gong, B., Zheng, Y. F., and Chen, R. X., 2007. TC/EA-MS online determination of hydrogen
1004 isotope composition and water concentration in eclogitic garnet. *Physics and*
1005 *Chemistry of Minerals* **34**, 687-698.
1006 Govindaraju, K. and Mevelle, G., 1987. Fully automated dissolution and separation methods
1007 for inductively coupled plasma atomic emission-spectrometry rock analysis –
1008 application to the determination of rare-earth elements. *Journal of Analytical Atomic*
1009 *Spectrometry* **2**, 615-621.
1010 Granet, M., Chabaux, F., Stille, P., Dosseto, A., France-Lanord, C., and Blaes, E., 2010. U-
1011 series disequilibria in suspended river sediments and implication for sediment transfer
1012 time in alluvial plains: The case of the Himalayan rivers. *Geochimica Et*
1013 *Cosmochimica Acta* **74**, 2851-2865.
1014 Granet, M., Chabaux, F., Stille, P., France-Lanord, C., and Pelt, E., 2007. Time-scales of
1015 sedimentary transfer and weathering processes from U-series nuclides: Clues from the
1016 Himalayan rivers. *Earth and Planetary Science Letters* **261**, 389-406.
1017 Heroy, D. C., Kuehl, S. A., and Goodbred, S., 2004. Mineralogy of the Ganges and
1018 Brahmaputra Rivers: implications for river switching and Late Quaternary climate
1019 change. *Sedimentary Geology* **155**, 343–359.
1020 Hilley, G. E., Chamberlain, C. P., Moon, S., Porder, S., and Willett, S. D., 2010. Competition

between erosion and reaction kinetics in controlling silicate-weathering rates. *Earth and Planetary Science Letters* **293**, 191-199.

HMG, 1994. His Majesty's Government of Nepal - Middle Marsyandi Hydroelectric Project, Nepal Electr. Author.

Huh, Y., 2010. Estimation of atmospheric CO2 uptake by silicate weathering in the Himalayas and the Tibetan Plateau: a review of existing fluvial geochemical data *Geological Society London Special Publications* **342**, 129-151.

Huyghe, P., Guilbaud, R., Bernet, M., Galy, A., and Gajurel, A. P., 2010. Significance of the clay mineral distribution in fluvial sediments of the Neogene to Recent Himalayan Foreland Basin (west-central Nepal). *Basin Research*, no-no.

Jacobson, A. D., Blum, J. D., and Walter, L. M., 2002. Reconciling the elemental and Sr isotope composition of Himalayan weathering fluxes; insights from the carbonate geochemistry of stream waters. *Geochimica et Cosmochimica Acta* **66**, 3417-3429.

Lave, J. and Avouac, J. P., 2000. Active folding of fluvial terraces across the Siwaliks Hills, Himalayas of central Nepal. *Journal of Geophysical Research, B, Solid Earth and Planets* **105**, 5735-5770.

Lavé, J. and Avouac, J. P., 2001. Fluvial incision and tectonic uplift across the Himalayas of central Nepal. *J. Geophys. Res.* **106**, 26561.

Lawrence, J. R. and Taylor, H. P., 1971. Deuterium and oxygen-18 correlation : clay minerals and hydroxides in quaternary soils compared to meteoric waters. *Geochimica et Cosmochimica Acta* **35**, 993-1003.

Lawrence, J. R. and Taylor, H. P., 1972. Hydrogen and oxygen isotope systematics in weathering profiles. *Geochimica Et Cosmochimica Acta* **36**, 1377-&.

Lupker, M., France-Lanord, C., Lavé, J., Bouchez, J., Galy, V., Métivier, F., Gaillardet, J., Lartiges, B., and J.-L. Mugnier, 2011. A Rouse-based method to integrate the

chemical composition of river sediments: application to the Ganga basin. *J. Geophys. Res*. doi : 10.1029/2010JF001947

Lyon-Caen, H. and Molnar, P., 1983. Constraints on the structure of the Himalaya from an analysis of gravity anomalies and a flexural model of the lithsophere. *Journal of Geophysical Research* **88**, 8171-8191.

Meade, R. H., Dunne, T., Richey, J. E., Santos, U. D., and Salati, E., 1985. Storage and remobilization of suspended sediment in the lower Amazon River of Brazil. *Science* **228**, 488-490.

Meybeck, M., 1987. Global chemical weathering of surficial rocks estimated from river dissolved loads. *American Journal of Science* **287**, 401-428.

Morse, J. W. and Arvidson, R. S., 2002. The dissolution kinetics of major sedimentary carbonate minerals. *Earth-Science Reviews* **58**, 51-84.

Oelkers, E. H. and Schott, J., 1995. Experimental study of anorthite dissolution and the relative mechanism of feldspar hydrolysis. *Geochimica Et Cosmochimica Acta* **59**, 5039-5053.

Paul, M., 2008. Etude des isotopes de l'osmium dans les eaux souterraines du Bangladesh et les sédiments himalayens: implications et rôle de l'érosion himalayenne sur le budget océanique de l'osmium., Doctorat Géosciences, INPL Nancy - France

Pecher, A., 1978. Deformation et metamorphisme associés à une zone de cisaillement. Exemple du grand chevauchement central himalayen (M.C.T.), transverale des Annapurnas et du Manaslu, Nepal. Thèse Sci., Grenoble, 354p.

Pokrovsky, O. S., Golubev, S. V., and Schott, J., 2005. Dissolution kinetics of calcite, dolomite and magnesite at 25 ∞C and 0 to 50 atm pCO2. *Chemical Geology* **217**, 239-255.

Rao, K. L., 1979. *India's water wealth*. Orient Longman limited, New Delhi.

1071 Raymo, M. E., Ruddiman, W. F., and Froelich, P. N., 1988. Influence of late Cenozoic
1072 mountain building on ocean geochemical cycles. *Geology* **16**, 649-653.
1073 Rengarajan, R., Singh, S. K., Sarin, M. M., and Krishnaswami, S., 2009. Strontium isotopes
1074 and major ion chemistry in the Chambal River system, India: Implications to silicate
1075 erosion rates of the Ganga. *Chemical Geology* **260**, 87-101.
1076 RSP, 1996. River Survey Project, Flood Action Plan (FAP) final report. Delft Hydraulics and
1077 DHI.
1078 Sanyal, P., Bhattacharya, S. K., and Prasad, M., 2005. Chemical diagenesis of Siwalik
1079 sandstone: Isotopic and mineralogical proxies from Surai Khola section, Nepal.
1080 *Sedimentary Geology* **180**, 57-74.
1081 Sarin, M. M., Krishnaswami, S., Dilli, K., Somayajulu, B. L. K., and Moore, W. S., 1989.
1082 Major ion chemistry of the Ganga-Brahmaputra river system: Weathering processes
1083 and fluxes to the Bay of Bengal. *Geochimica et Cosmochimica Acta* **53**, 997-1009.
1084 Savin, S. M. and Epstein, S., 1970. Oxygen and hydrogen isotope geochemistry of lcay
1085 minerals. *Geochimica Et Cosmochimica Acta* **34**, 25-&.
1086 Sharp, Z. D., Atudorei, V., and Durakiewicz, T., 2001. A rapid method for determination of
1087 hydrogen and oxygen isotope ratios from water and hydrous minerals. *Chemical*
1088 *Geology* **178**, 197-210.
1089 Sheppard, S. M. F. and Schwarcz, H. P., 1970. Fractionation of carbon and oxygen isotopes
1090 and magnesium between coexisting metamorphic calcite and dolomite. *Contributions*
1091 *to Mineralogy and Petrology* **26**, 161-198.
1092 Singh, M., Sharma, M., and Tobschall, H. J., 2005. Weathering of the Ganga alluvial plain,
1093 northern India: implications from fluvial geochemistry of the Gomati River. *Applied*
1094 *Geochemistry*, 1-21.
1095 Singh, S. K., Rai, S. K., and Krishnaswami, S., 2008. Sr and Nd isotopes in river sediments

from the Ganga Basin: Sediment provenance and spatial variability in physical erosion. *J. Geophys. Res.* **113**, F03006.

Sinha, R. and Friend, P. F., 1994. River systems and their sediment flux, Indo-Gangetic plains, northern Bihar, India. *Sedimentology* **41**, 825-845.

Sinha, R., Kettanah, Y., Gibling, M. R., Tandon, S. K., Jain, M., Bhattacharjee, P. S., Dasgupta, A. S., and Ghazanfari, P., 2009. Craton-derived alluvium as a major sediment source in the Himalayan Foreland Basin of India. *Geological Society of America Bulletin* **121**, 1596-1610.

Sinha, R., Tandon, S. K., Sanyal, P., Gibling, M. R., Stuben, D., Berner, Z., and Ghazanfari, P., 2006. Calcretes from a Late Quaternary interfluve in the Ganga Plains, India: Carbonate types and isotopic systems in a monsoonal setting. *Palaeogeography, Palaeoclimatology, Palaeoecology* **242**, 214-239.

Srivastava, P., Singh, I. B., Sharma, M., and Singhvi, A. K., 2003. Luminescence chronometry and Late Quaternary geomorphic history of the Ganga Plain, India. *Palaeogeography, Palaeoclimatology, Palaeoecology* **197**, 15-41.

Szramek, K., McIntosh, J. C., Williams, E. L., Kanduc, T., Ogrinc, N., and Walter, L. M., 2007. Relative weathering intensity of calcite versus dolomite in carbonate-bearing temperate zone watersheds: Carbonate geochemistry and fluxes from catchments within the St. Lawrence and Danube river basins. *Geochem. Geophys. Geosyst.* **8**, Q04002.

Tomar, K. P., 1987. Chemsitry of pedogenesis in Indo-Gangetic alluvial plains. *Journal of Soil Science* **38**, 405-414.

Van Der Beek, P., Robert, X., Mugnier, J.-L., Bernet, M., Huyghe, P., and Labrin, E., 2006. Late Miocene ? Recent exhumation of the central Himalaya and recycling in the foreland basin assessed by apatite fission-track thermochronology of Siwalik

1121 sediments, Nepal. *Basin Research* **18**, 413-434.
1122 Vance, D., Bickle, M., Ivy-Ochs, S., and Kubik, P. W., 2003. Erosion and exhumation in the
1123 Himalaya from cosmogenic isotope inventories of river sediments. *Earth and*
1124 *Planetary Science Letters* **206**, 273-288.
1125 Velde, B. B. and Meunier, A., 2008. The Origin of Clay Minerals in Soils and Weathered
1126 Rocks. Springer.
1127 Walker, J. C. G., Hays, P. B., and Kasting, J. F., 1981. A negative feed back mechanism for
1128 the long-term stabilization of Earth's surface temperature. *Journal of Geophysical*
1129 *Research* **86**, 9776-9782.
1130 WARPO, Water Resources Planning Organization, Ministry of water resources, Government
1131 of the People's Republic of Bangladesh. Hydrological data.
1132 West, A. J., Bickle, M. J., Collins, R., and Brasington, J., 2002. Small-catchment perspective
1133 on Himalayan weathering fluxes. *Geology* **30**, 355-358.
1134 West, A. J., Galy, A., and Bickle, M., 2005. Tectonic and climatic controls on silicate
1135 weathering. *Earth and Planetary Science Letters* **235**, 211-228.
1136 White, A. F. and Brantley, S. L., 2003. The effect of time on the weathering of silicate
1137 minerals: why do weathering rates differ in the laboratory and field? *Chemical*
1138 *Geology* **202**, 479-506.
1139 Wilson, M. J., 2004. Weathering of the primary rock-forming minerals: processes, products
1140 and rates. *Clay Minerals* **39**, 233-266.
1141 Yadav, S., Chakrapani, G., and Gupta, M., 2008. An experimental study of dissolution
1142 kinetics of Calcite, Dolomite, Leucogranite and Gneiss in buffered solutions at
1143 temperature 25 and 5°C. *Environmental Geology* **53**, 1683-1694.
1144 Yapp, C. J. and Pedley, M. D., 1985. Stable Hydrogen isotopes in iron-oxides. 2. D/H
1145 variations among natural Goethites. *Geochimica Et Cosmochimica Acta* **49**, 487-495.
1146

Figures

Figure 1: Geographical setting of the Ganga basin showing the main sample sites and corresponding sample numbers. A geological sketch of the main Himalayan faults zones is also shown (ITS: Indus-Tsangpo Suture; STD: South Tibetan Detachment; MCT: Main Central Thrust; MBT: Main Boundary Thrust; MFT: Main Frontal Thrust).

Figure 2: Evolution of sediment concentration in the water column of the Ganga in Bangladesh (BR 511 - 516) along with the evolution of the chemical composition of major elements Si, Al, Fe, Na, K as well as H_2O^+. Mineral sorting within the water column is a first order control on the chemical composition of sampled sediments (Lupker et al., 2011; Bouchez et al., 2011b).

Figure 3: Schematic evolution of the sedimentary load during transfer from the Himalayan front downstream to the Ganga in Bangladesh. (a) Sediment hydrodynamic sorting results in mixing trend between coarse grained, quartz rich, low Al/Si sediments and a clay and phyllosilicate rich end-member. Weathering is marked by a loss of mobile elements (e.g. K, Na, …) relative to Si at constant Al/Si. (b) Sediment sequestration in the floodplain results in a relative increase of the average Al/Si ratio of the total transported sediment load. This evolution is however limited for the Ganga as at the Himalayan front the average Al/Si is ca. 0.22 and in the Ganga in Bangladesh this ratio is estimated at ca. 0.23 (Lupker et al., 2011).

Figure 4: a. Evolution of the Fe/Si ratio as a function of the Al/Si ratio, proxy for grain-size and mineral sorting in the river water column. Himalayan Rivers form a relatively uniform trend that is markedly different from sediments from the southern tributaries such as the

Chambal. This difference can be used to trace inputs from Chambal sediments in sediments from the Ganga mainstream. **b.** Detailed graph of the Himalayan front rivers. **c.** Temporal of Fe/Si ratios of sediments sampled in the Ganga in Bangladesh, plotted as a function of sampling year, highlighting the heterogeneity of the exported chemical signal.

Figure 5: a. Evolution of the Na/Si ratio as a function of the Al/Si ratio, showing a depletion in Na relative to Si from the Himalayan front Rivers (black squares) downstream to the Himalayan floodplain Rivers (light grey diamonds) and the Ganga in Bangaldesh (open circles). **b.** Composition variability amongst Himalayan front Rivers showing a Na-depleted Karnali compared to other Himalayan Rivers **c.** Inter-annual variability of the Na/Si ratio in Ganga sediments sampled in Bangladesh.

Figure 6: Evolution of the K/Si ratio as a function of the Al/Si ratio, showing a depletion in K from the Himalayan front Rivers (black squares) downstream to the Himalayan floodplain Rivers (light grey diamonds) and the Ganga in Bangaldesh (open circles). **b.** Himalayan front River sediments have homogeneous K/Si composition **c.** Inter-annual variability of the K/Si ratio in Ganga sediments sampled in Bangladesh.

Figure 7: Evolution of the H_2O^+/Si ratio as a function of the Al/Si ratio. **a.** Evolution of H_2O^+/Si from the Himalayan front rivers (black squares), further downstream upon floodplain transfer (light grey diamonds) compared to Ganga sediments sampled in Bangladesh (open circles) and the major southern contribution of the Chambal (black triangles). **b.** Detailed plot of the evolution of Himalayan rivers upon floodplain transfer. **c.** Inter-annual variability of the H_2O^+/Si ratio in Ganga sediments sampled in Bangladesh.

Figure 8: D/H isotopic composition of bulk sediments from the Ganga basin as a function of hydration expressed as the H_2O^+/Al ratio. The hydration and isotopic composition of muscovite, biotite and vermiculite separated from Himalayan sediments (see supplementary data file, Table S2) is also plotted for references.

Figure 9: Calcite and dolomite content of sediments from the Ganga basin.

Figure 10: Oxygen and carbon isotopic composition of calcite (a) and dolomite (b) of river sediments from the Ganga basin. The range of composition of pedogenic carbonates from the northeastern Ganga floodplain (Sinha et al., 2006), Siwaliks carbonates from the Surai Khola section in Nepal (Suppelmentary data file, Table S3; Sanyal et al., 2005), biogenic shells from the Gangetic plain (Gajurel et al., 2006) and Himalayan source rocks (Galy et al., 1999) is also shown.

Figure 11: Mg^s/Si (a) and Ca^s/Si ratio (b) as a function of Al/Si ratio for river sediments from the Himalayan front Rivers, the Himalayan flood plain Rivers, the Ganga in Bangladesh, the Chambal and Gomti Rivers. Mg^s and Ca^s are derived from the sediment bulk Mg and Ca content after correction for calcite and dolomite Ca and Mg contribution.

Figure 12: Na/Si, K/Si and H_2O^+/Si ratios of the main lithological units of the Himalayan orogen: Siwaliks, Lesser Himalaya (LH) and High Himalaya Cristalines (HHC). The chemical composition of these units are from Galy and France-Lanord (2001) and Lupker et al. (2011) and are based on outcrop samples.

Figure 13: Evolution of the normalized mobile element composition of sediments in the Himalayan system. Weathering in the Himalayan range (green envelope) is computed for an average Al/Si ratio of 0.22. Weathering in the floodplain (red envelope) is determined for an average Al/Si ratio of sediments of 0.23 as sequestration in the floodplain leads to an increase in the average Al/Si ratio. For carbonates the Si normalized ratios were determined by averaging all available data for each considered river as carbonate content does not show any relation to Al/Si. Gomti River sediments as potential analogue for floodplain material are also shown for comparison. Details on the calculation can be found in Appendix B.

Figure 1:

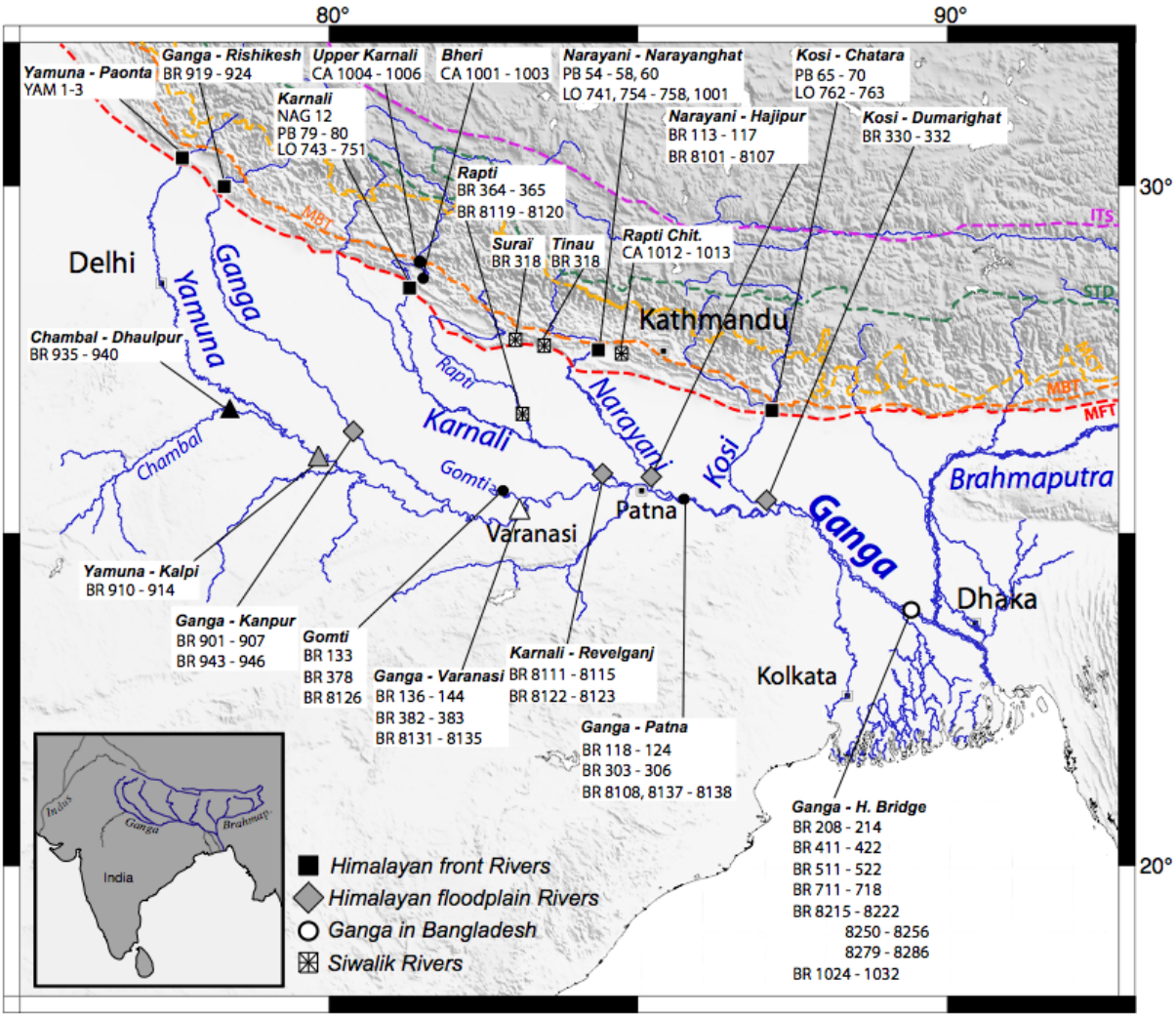
80°
90°
30°
20°
Yamuna - Paonta
YAM 1-3
Ganga - Rishikesh
BR 919 - 924
Upper Karnali
CA 1004 - 1006
Bheri
CA 1001 - 1003
Narayani - Narayanghat
PB 54 - 58, 60
LO 741, 754 - 758, 1001
Kosi - Chatara
PB 65 - 70
LO 762 - 763
Karnali
NAG 12
PB 79 - 80
LO 743 - 751
Narayani - Hajipur
BR 113 - 117
BR 8101 - 8107
Kosi - Dumarighat
BR 330 - 332
Rapti
BR 364 - 365
BR 8119 - 8120
Surai
BR 318
Tinau
BR 318
Rapti Chit.
CA 1012 - 1013
Chambal - Dhaulpur
BR 935 - 940
Yamuna - Kalpi
BR 910 - 914
Ganga - Kanpur
BR 901 - 907
BR 943 - 946
Gomti
BR 133
BR 378
BR 8126
Ganga - Varanasi
BR 136 - 144
BR 382 - 383
BR 8131 - 8135
Karnali - Revelganj
BR 8111 - 8115
BR 8122 - 8123
Ganga - Patna
BR 118 - 124
BR 303 - 306
BR 8108, 8137 - 8138
Ganga - H. Bridge
BR 208 - 214
BR 411 - 422
BR 511 - 522
BR 711 - 718
BR 8215 - 8222
8250 - 8256
8279 - 8286
BR 1024 - 1032
Delhi
Yamuna
Ganga
Kathmandu
Chambal
Rapti
Karnali
Narayani
Kosi
Gomti
Varanasi
Patna
Brahmaputra
Ganga
Dhaka
Kolkata
MBT
MFT
ITS
STD
India
Himalayan front Rivers
Himalayan floodplain Rivers
Ganga in Bangladesh
Siwalik Rivers

1234 **Figure 2:**

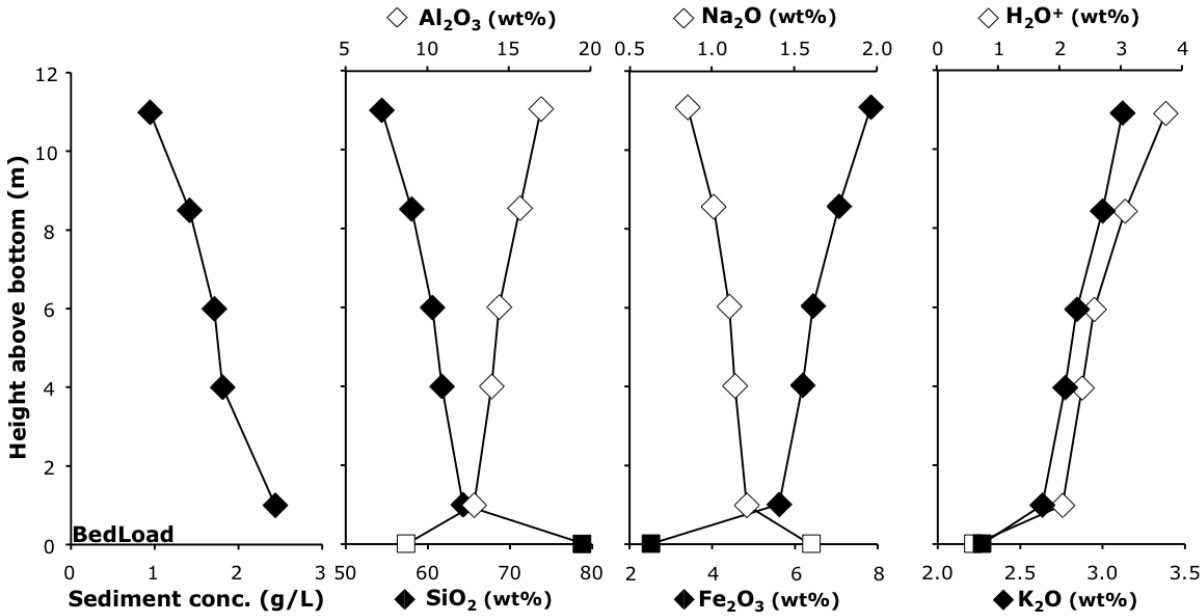

1235

1236

Figure 3:

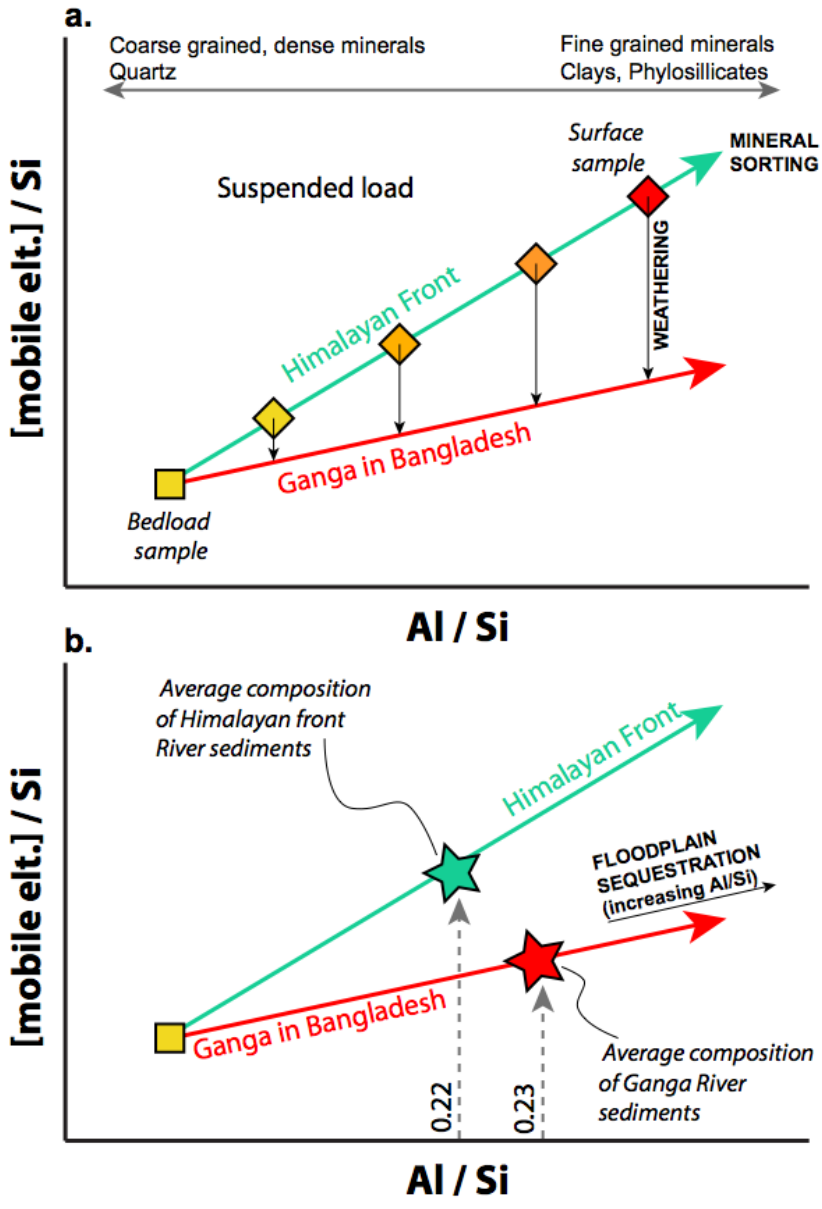
a.
Coarse grained, dense minerals
Quartz
Fine grained minerals
Clays, Phylosillicates
Surface
sample
MINERAL
SORTING
Suspended load
WEATHERING
Himalayan Front
Ganga in Bangladesh
Bedload
sample
[mobile elt.] / Si
Al / Si
b.
Average composition
of Himalayan front
River sediments
Himalayan Front
FLOODPLAIN
SEQUESTRATION
(increasing Al/Si)
Ganga in Bangladesh
Average composition
of Ganga River
sediments
0.22
0.23
[mobile elt.] / Si
Al / Si

1239 **Figure 4:**

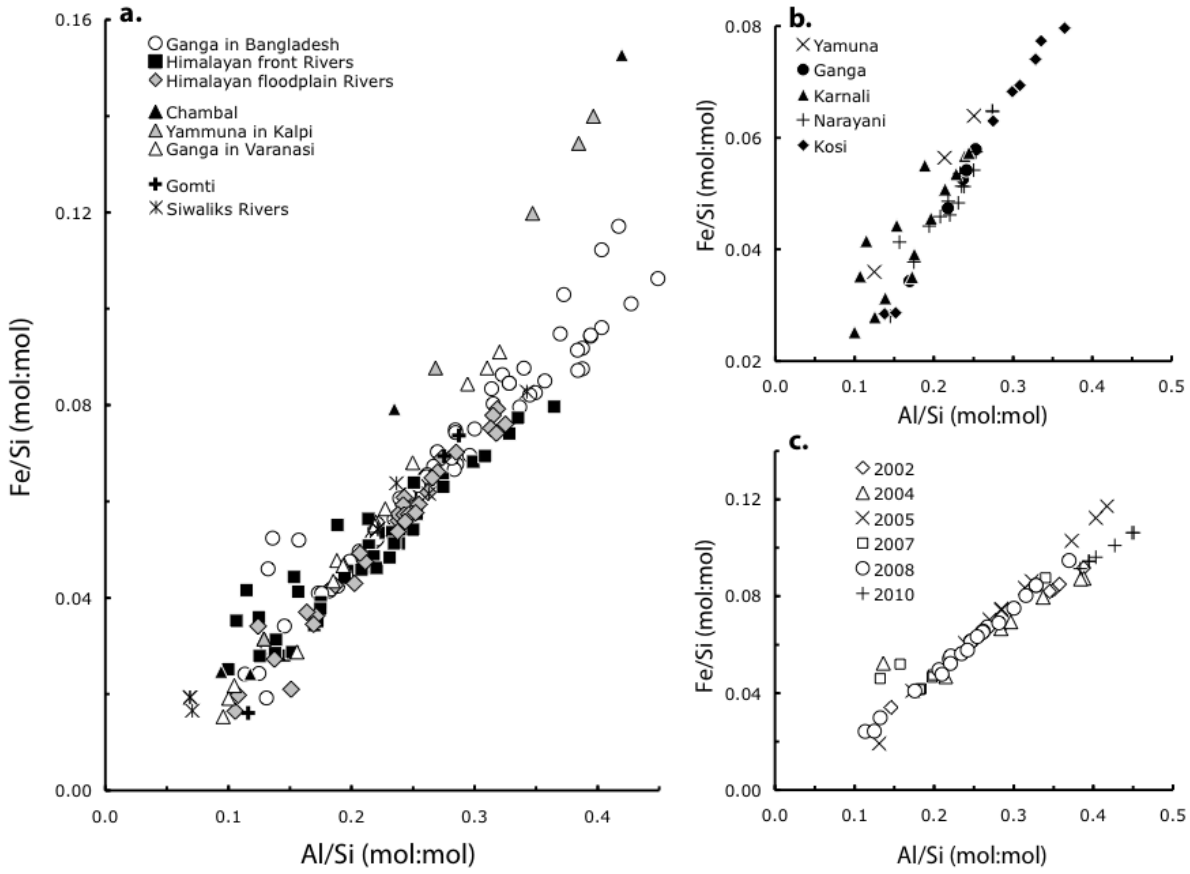

1240

1241

Figure 5:

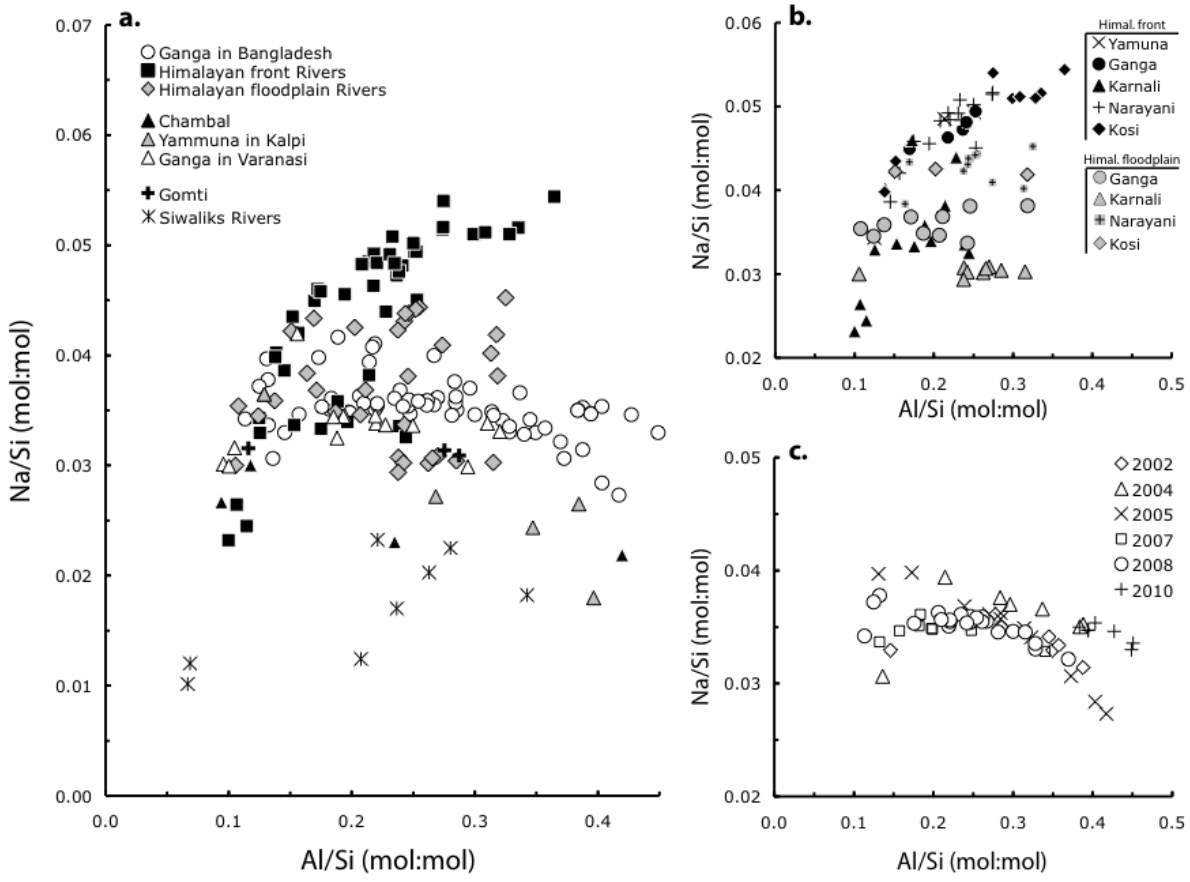
a.
Ganga in Bangladesh
Himalayan front Rivers
Himalayan floodplain Rivers
Chambal
Yammuna in Kalpi
Ganga in Varanasi
Gomti
Siwaliks Rivers
Na/Si (mol:mol)
Al/Si (mol:mol)
b.
Himal. front
Yamuna
Ganga
Karnali
Narayani
Kosi
Himal. floodplain
Ganga
Karnali
Narayani
Kosi
Na/Si (mol:mol)
Al/Si (mol:mol)
c.
2002
2004
2005
2007
2008
2010
Na/Si (mol:mol)
Al/Si (mol:mol)

1244 **Figure 6:**

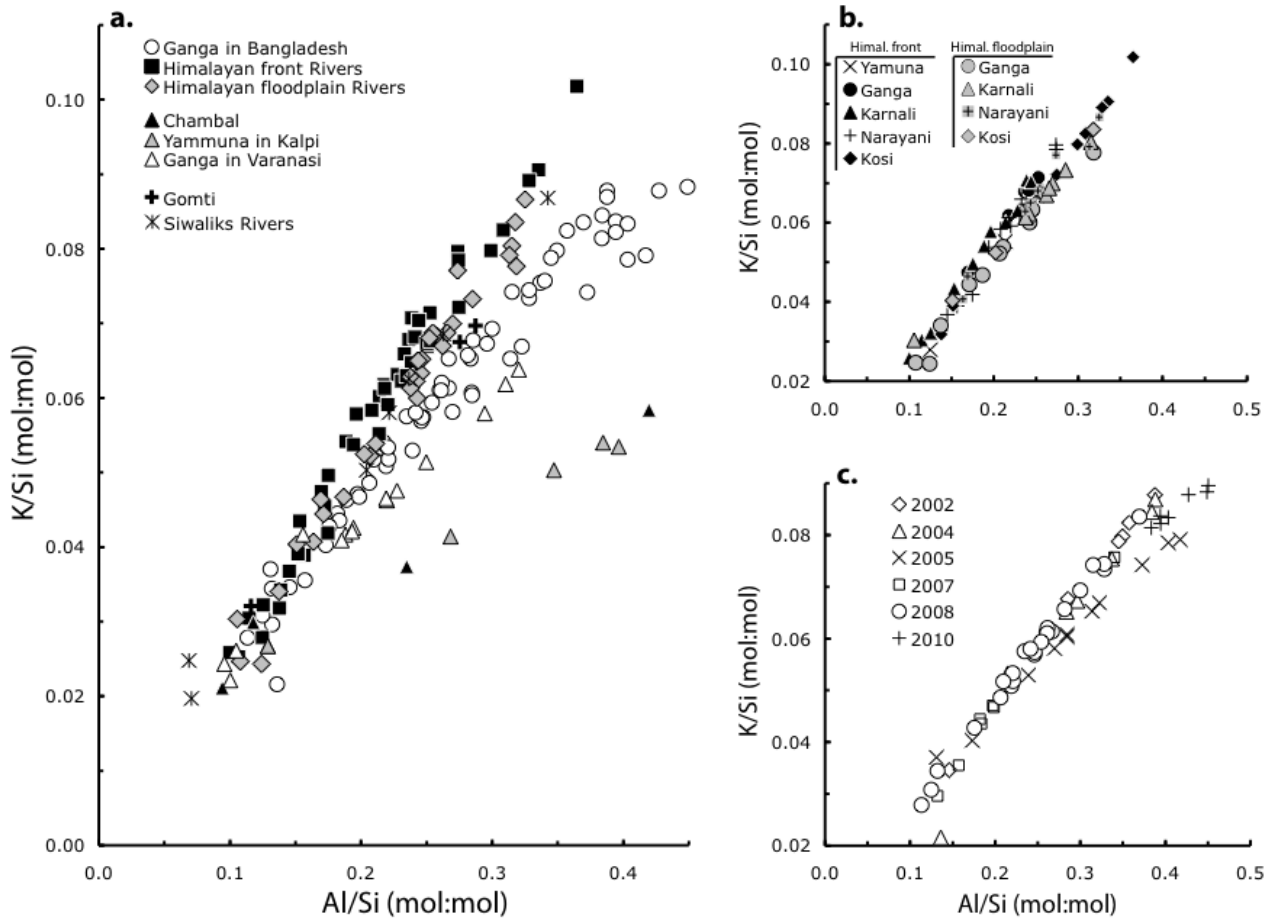

1245

1246

1247 **Figure 7:**

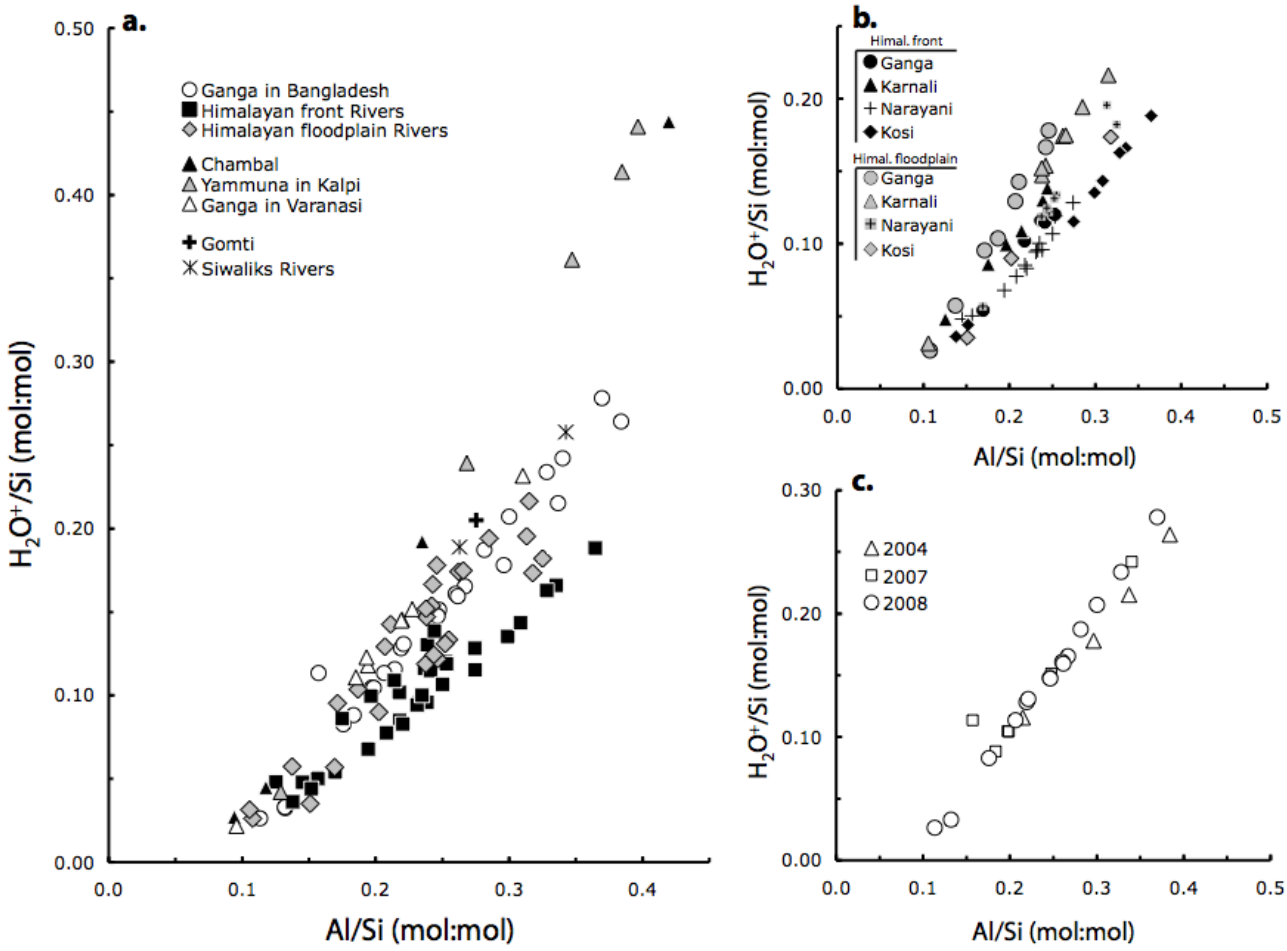

1248

1249 **Figure 8:**

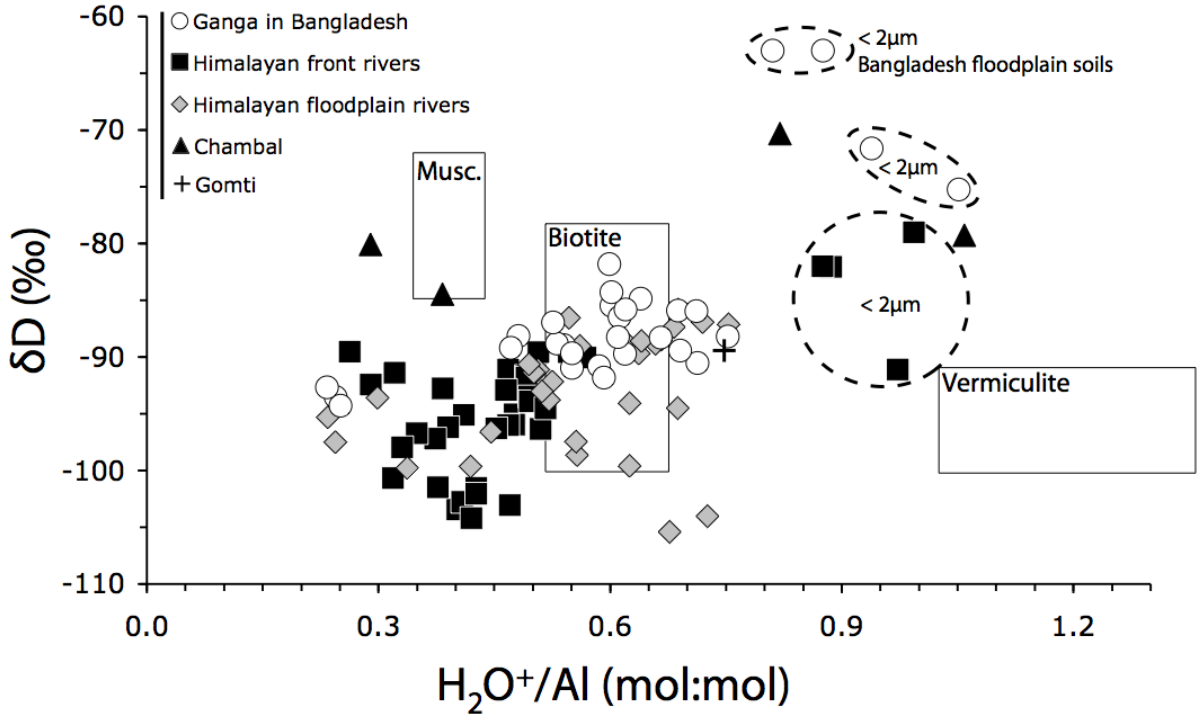

1250

Figure 9:

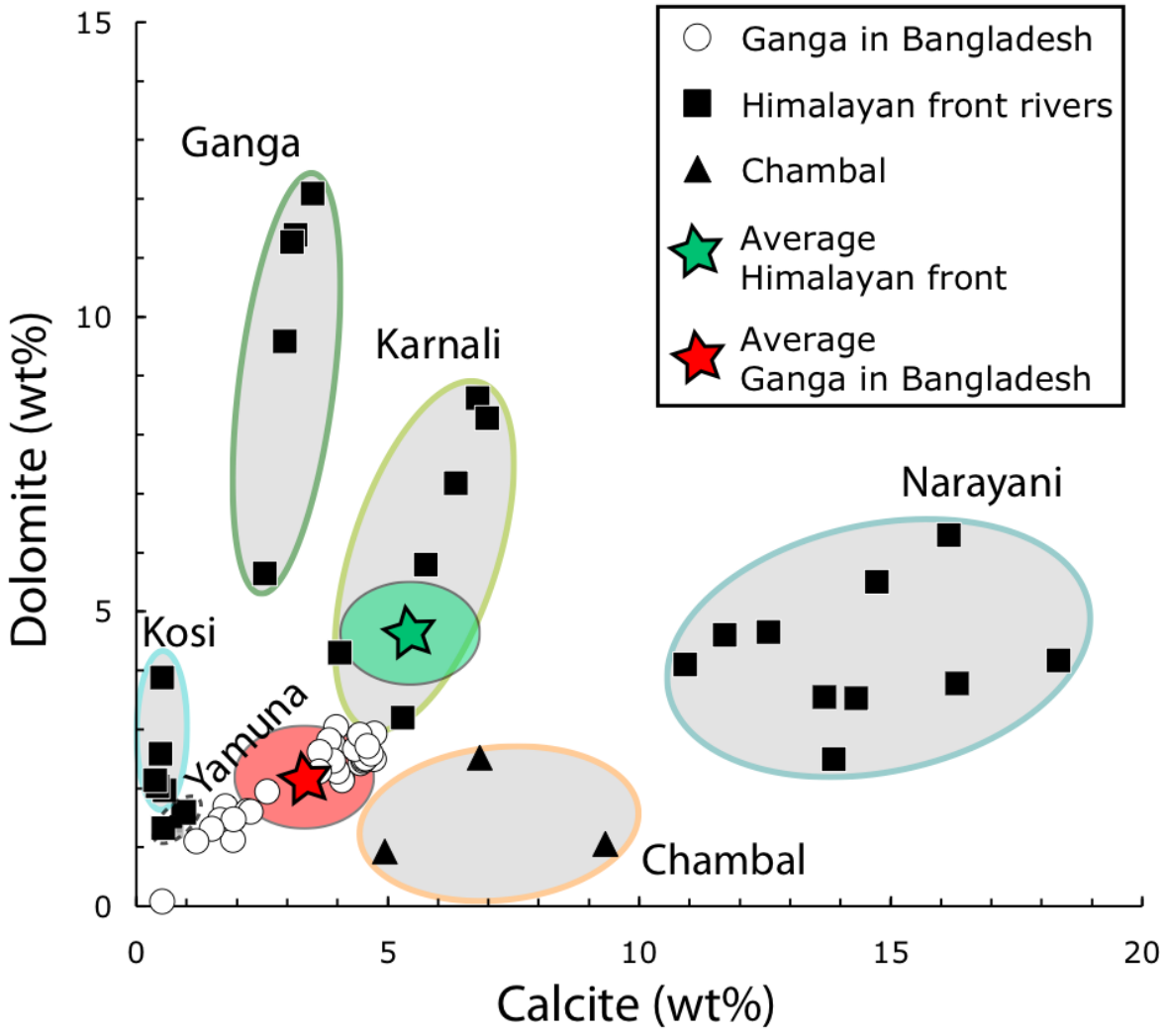
Ganga in Bangladesh
Himalayan front rivers
Chambal
Average Himalayan front
Average Ganga in Bangladesh
Ganga
Karnali
Narayani
Kosi
Yamuna
Chambal
Dolomite (wt%)
Calcite (wt%)
0
5
10
15
20

Figure 10:

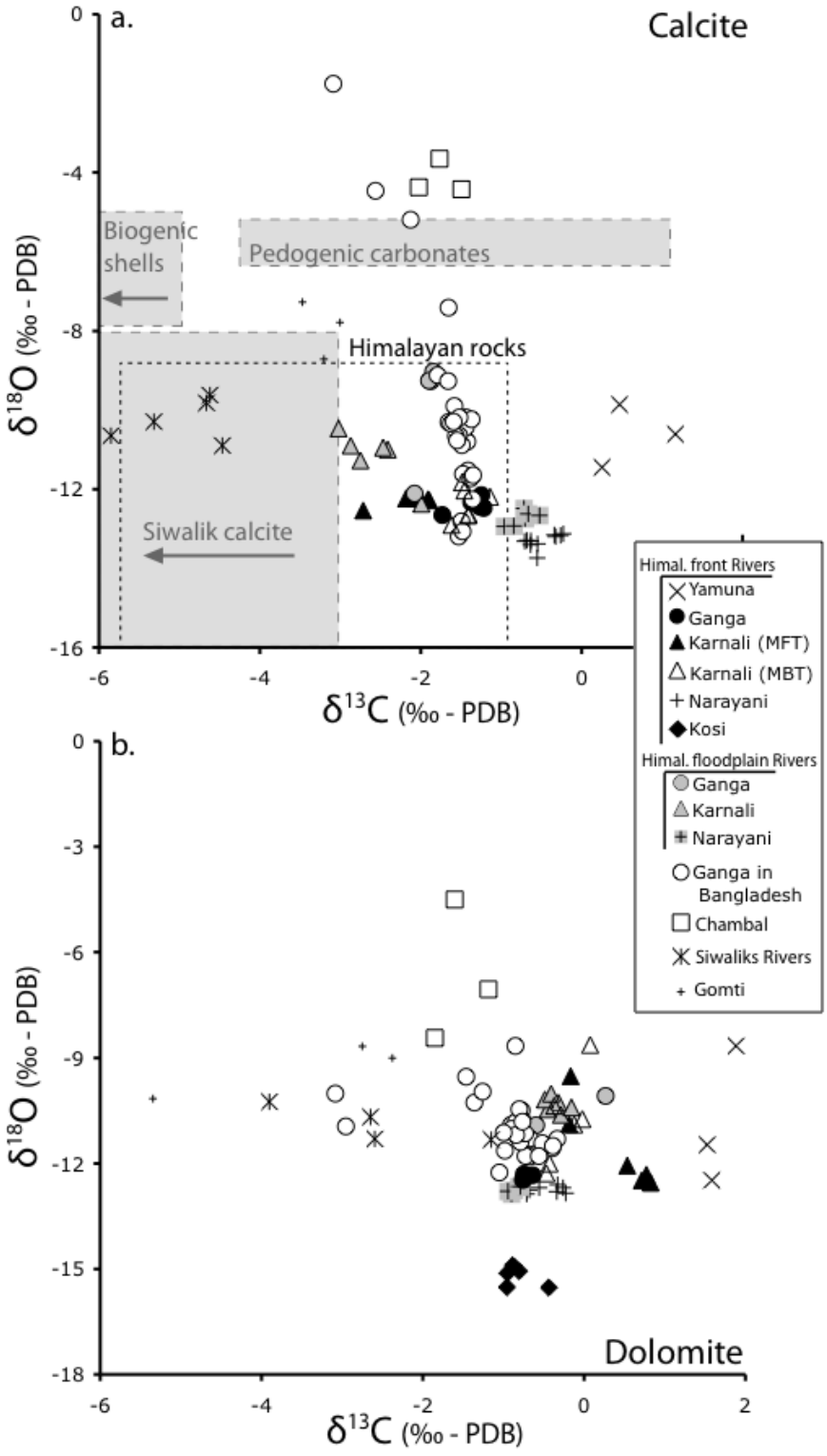
a.
Calcite
Biogenic shells
Pedogenic carbonates
Himalayan rocks
Siwalik calcite
δ18O (‰ - PDB)
δ13C (‰ - PDB)
0
-4
-8
-12
-16
-6
-4
-2
0
Himal. front Rivers
Yamuna
Ganga
Karnali (MFT)
Karnali (MBT)
Narayani
Kosi
Himal. floodplain Rivers
Ganga
Karnali
Narayani
Ganga in Bangladesh
Chambal
Siwaliks Rivers
Gomti
b.
0
-3
-6
-9
-12
-15
-18
-6
-4
-2
0
2
Dolomite
δ18O (‰ - PDB)
δ13C (‰ - PDB)

1256 **Figure 11:**

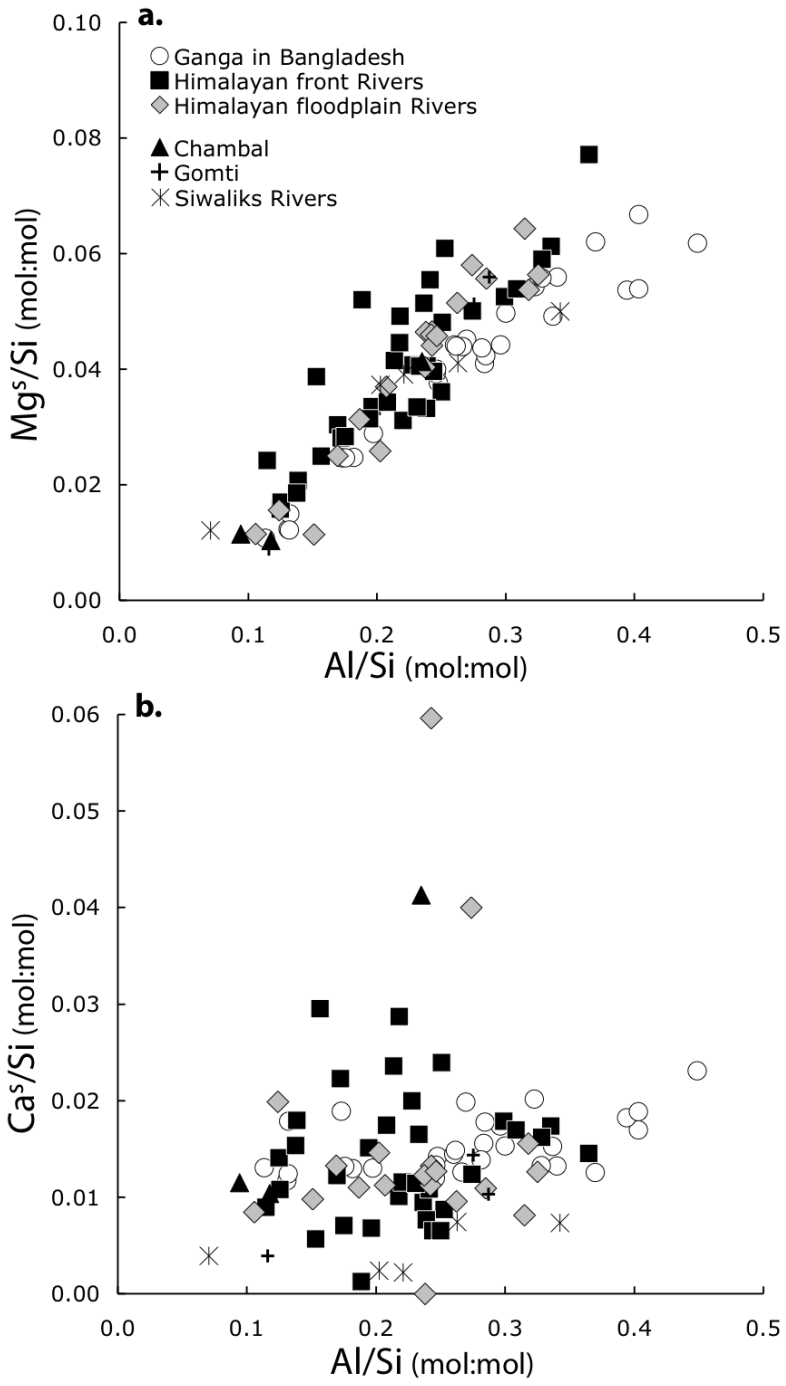

1257

Figure 12:

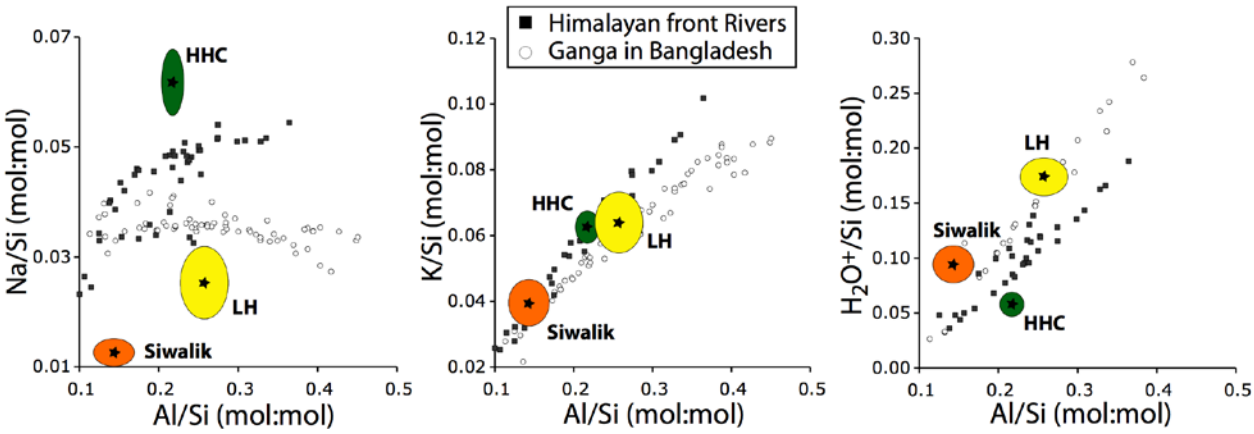
Himalayan front Rivers
Ganga in Bangladesh
HHC
LH
Siwalik
Na/Si (mol:mol)
K/Si (mol:mol)
H2O+/Si (mol:mol)
Al/Si (mol:mol)
0.07
0.05
0.03
0.01
0.12
0.10
0.08
0.06
0.04
0.02
0.30
0.25
0.20
0.15
0.10
0.05
0.00
0.1
0.2
0.3
0.4
0.5

Figure 13:

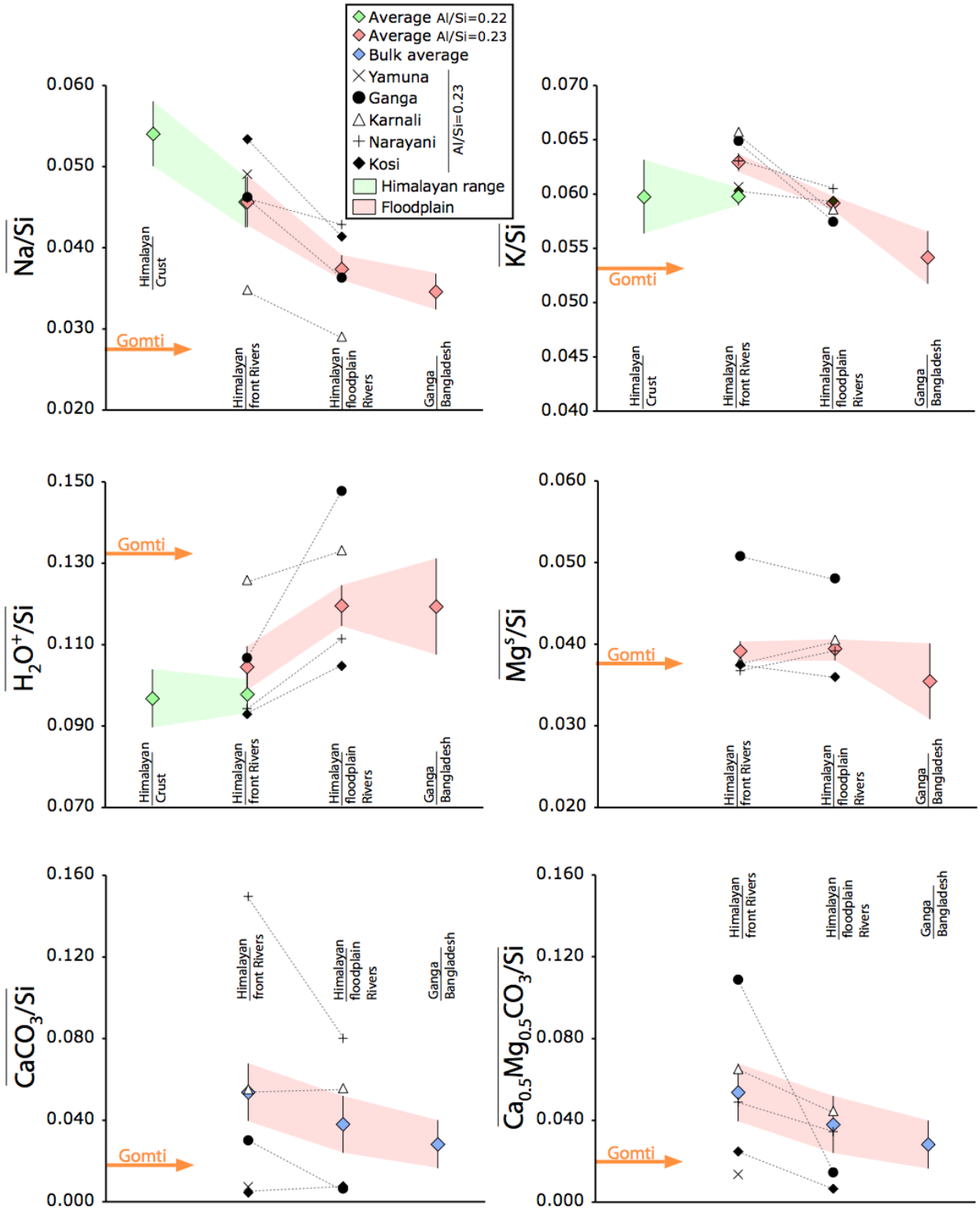
Average Al/Si=0.22
Average Al/Si=0.23
Bulk average
Yamuna
Ganga
Karnali
Narayani
Kosi
Al/Si=0.23
Himalayan range
Floodplain
Na/Si
K/Si
H_2O^+/Si
Mg^s/Si
$CaCO_3/Si$
$Ca_{0.5}Mg_{0.5}CO_3/Si$
Gomti
Himalayan Crust
Himalayan front Rivers
Himalayan floodplain Rivers
Ganga Bangladesh

Tables:

Table 1: Major elements distribution in the water column and main mineralogical species contributing to the different elements in the Ganga basin. Mineralogical data based on analysis mineral separates from Ganga sediments (Garzanti et al., 2011).

Table 2: $\Delta\overline{X/Si}$ as computed from equation (2) showing the depletion in mobile elements relative to silicon for the different compartments of the Ganga basin. Negative values denote gain of mobile elements.

Table 3: Weathering flux generated in the Ganga floodplain as computed from the river sediments according to equation (4). [1]Sediment derived weathering fluxes are compared to the dissolved load of the Ganga in Bangladesh (corrected for cyclic contributions) estimated by Galy and France-Lanord (1999).

1277 **Table 1:**

	Si	Al	Fe	Na	K	Ca	Mg	H_2O^+
Enrichment in water column	bottom	surface	surface	bottom	surface	n.d.	surface	surface
Carrying mineral	Quartz Feldspar Mica	Mica Feldspar Clay	Biotite Clay Fe-hydrox. Opaques	Albite Other feldspar	Mica K-feldspar	Calcite Dolomite Plagioclase	Mica Dolomite	Mica Clay Fe-hydrox.

1278

1279

1280

1281 **Table 2:**

	Himalayan Range	Floodplain N	Floodplain S	Total floodplain
$\Delta Na/Si$	0.008 (±0.008)	0.008 (±0.003)	0.003 (±0.003)	0.011 (±0.004)
$\Delta K/Si$	0.000 (±0.008)	0.004 (±0.001)	0.005 (±0.003)	0.009 (±0.003)
$\Delta H_2O^+/Si$	0.000 (±0.016)	-0.015 (±0.007)	0.000 (±0.013)	-0.015 (±0.013)
$\Delta Mg^s/Si$	-	0.000 (±0.002)	0.004 (±0.005)	0.004 (±0.005)
$\Delta CaCO_3/Si$	-	0.015 (±0.020)	0.010 (±0.018)	0.025 (±0.018)
$\Delta(Ca,Mg)CO_3/Si$	-	0.024 (±0.009)	0.004 (±0.010)	0.029 (±0.009)

1282

1283

1284 **Table 3:**

	10^9 mol/yr	% of total dissolved load[1]
φ **Na**	53 (±18)	70 %
φ **K**	42 (±13)	140 %
φ **H_2O^+**	-71 (±62)	-
φ **Silicate Mg**	17 (±23)	-
φ **Carbonate Mg**	69 (±22)	-
φ **Total Mg**	86 (±32)	100 %
φ **Silicate Ca**	*< 10*	-
φ **Carbonate Ca**	189 (±92)	-
φ **Total Ca**	199 (±100)	98 %

1285